



OPEN

Tyrosinase-mediated synthesis of larvicidal active 1,5-diphenyl pent-4-en-1-one derivatives against *Culex quinquefasciatus* and investigation of their ichthyotoxicity

SathishKumar Chidambaram¹, Daoud Ali², Saud Alarifi², Raman Gurusamy³, SurendraKumar Radhakrishnan¹ & Idhayadhulla Akbar¹✉

1,5-diphenylpent-4-en-1-one derivatives were synthesised using the grindstone method with Cu(II)-tyrosinase used as a catalyst. This method showed a high yield under mild reaction conditions. The synthesised compounds were identified by FTIR, ¹H NMR, ¹³C NMR, mass spectrometry, and elemental analysis. In this study, a total of 17 compounds (1a–1q) were synthesised, and their larvicidal and antifeedant activities were evaluated. Compound 1i (1-(5-oxo-1,5-diphenylpent-1-en-3-yl)-3-(3-phenylallylidene)thiourea) was notably more active (LD₅₀: 28.5 μM) against *Culex quinquefasciatus* than permethrin (54.6 μM) and temephos (37.9 μM), whereas compound 1i at 100 μM caused 0% mortality in *Oreochromis mossambicus* within 24 h in an antifeedant screening, with ichthyotoxicity determined as the death ratio (%) at 24 h. Compounds 1a, 1e, 1f, 1j, and 1k were found to be highly toxic, whereas 1i was not toxic in antifeedant screening. Compound 1i was found to possess a high larvicidal activity against *C. quinquefasciatus* and was non-toxic to non-target aquatic species. Molecular docking studies also supported the finding that 1i is a potent larvicide with higher binding energy than the control (– 10.0 vs. – 7.6 kcal/mol) in the 3OGN protein. Lead molecules are important for their larvicidal properties and application as insecticides.

In the broadest sense, human beings are part of nature; however, our activity is often understood and interpreted as a category that is unique and separate from the rest of the natural phenomena. It is both the legal and moral obligation of every human to protect planet Earth by undertaking activities that would prevent contamination of our planet and thereby protect it for future generations. For instance, as a scientist in chemical industries or academia, one could focus on protecting nature by employing green chemistry to produce various chemical and pharmaceutical active ingredients. Of the several green chemistry methodologies, the grindstone chemistry technique is a simple practice for the preparation of chemical compounds. Toda et al. developed a range of chemical reactions carried out by simply grinding or triturating the solids together¹. We will now focus on Mannich reactions, which are a widely studied type of reaction in the organic and medicinal chemistry domains².

Mushroom tyrosinase, which has a dinuclear copper active centre, catalyses the hydroxylation and subsequent oxidation reactions that convert phenol to the related ortho-quinone as well as the oxidation of catechol to quinone^{3–8}. Tyrosinase, alongside catechol oxidase⁹ and hemocyanin¹⁰, belongs to the type 3 copper protein class. The dicopper core of this type-3 copper protein takes three redox forms^{3–8}. The active core of the deoxy type [Cu(I)–Cu(I)] contains two cuprous ions, which attach dioxygen to produce the oxy form. Dioxygen bonds as a peroxide ion in the oxy form in the μ-η²:η² side-on bridging mode [Cu(II)–O₂²⁻–Cu(II)]. The met type [Cu(II)–Cu(II)] signifies a condition wherein copper atoms only at the active site have been oxidised but have

¹Research Department of Chemistry, Nehru Memorial College (Affiliated to Bharathidasan University), Puthanampatti, Tiruchchirappalli District, Tamil Nadu 621007, India. ²Department of Zoology, College of Sciences, King Saud University (KSU), P.O. Box 2455, Riyadh 11451, Saudi Arabia. ³Department of Life Sciences, Yeungnam University, Gyeongsan 38541, Gyeongsan-buk, South Korea. ✉email: a.idhayadhulla@gmail.com

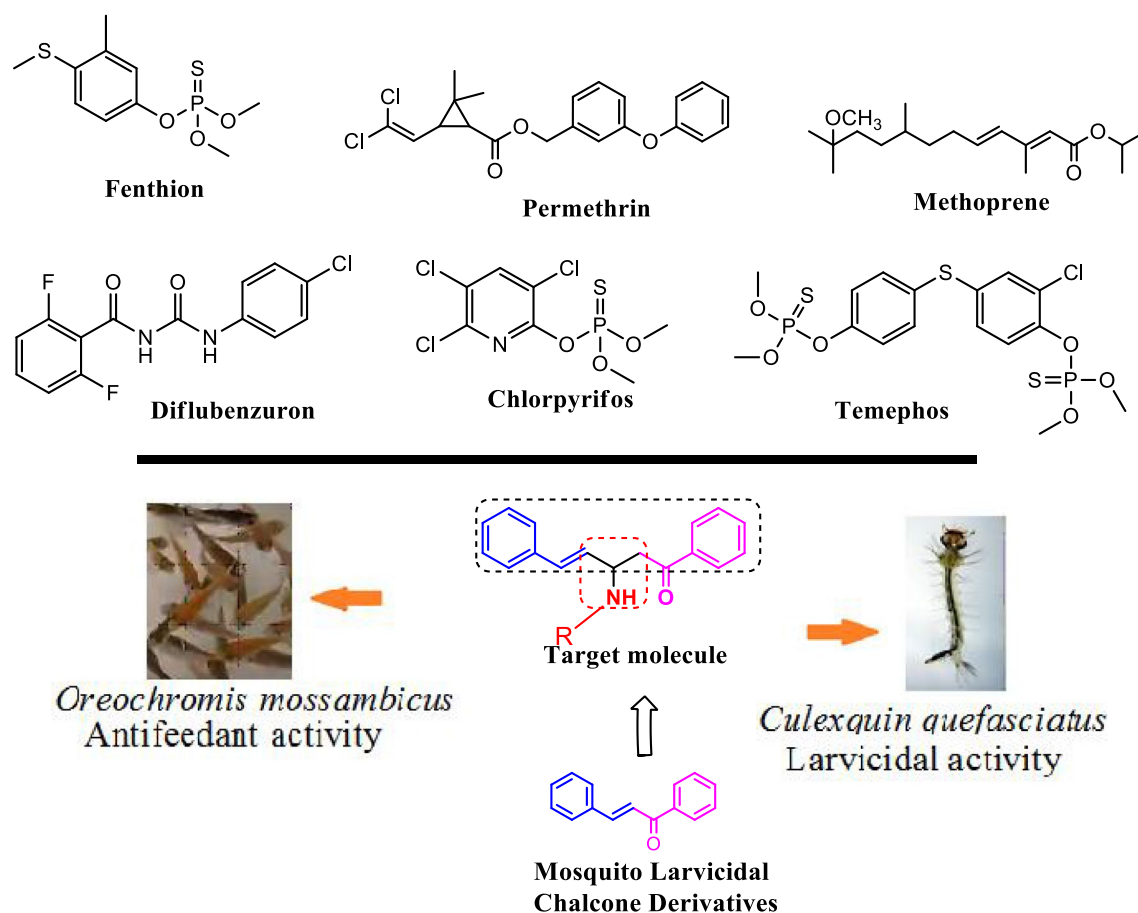


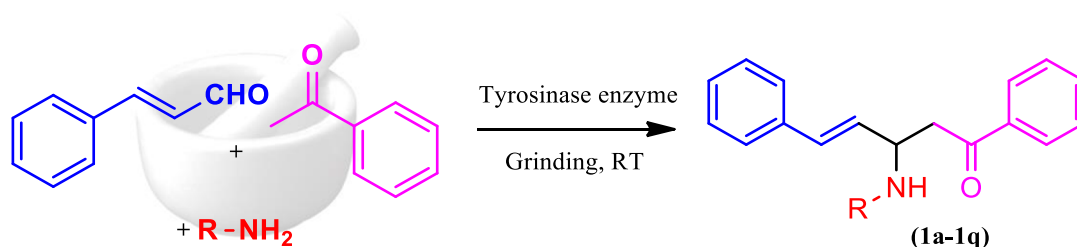
Figure 1. Synthetic marketable insecticides and our target molecule drawn by ChemDraw Ultra 12.0 Suite (PerkinElmer, USA).

not been bound by dioxygen. The met type of tyrosinase is an enzymatic form wherein two cupric ions are bridged by one or two tiny ligands, along with water molecules or hydroxide ions, while the enzyme is at rest and acting as a catalyst.

Mannich-type reactions face significant challenges in terms of reaction time, reaction conditions, toxicity, catalyst requirements, and separation and determination of the purity of final product(s). Other challenges include synthetic methodologies such as ultrasound or microwave irradiation, the use of Lewis acids or bases, and the use of solubilizing agents or surfactant-type catalysts¹¹. In addition, some of the known green trends in Mannich reactions consist of ball milling without solvents¹², using ionic liquid mediums¹³, using ionic liquids reinforced with nanoparticles¹⁴, or applying enzymes under bio-catalytic conditions^{15,16}. However, the present study focused on the grindstone green chemistry method in order to overcome the abovementioned challenges in the preparation of Mannich base derivatives.

Mosquitoes are an important transmission vector for several diseases, particularly malaria^{17,18}. These types of diseases have economic and social impacts worldwide. Among the mosquito species, *Culex quinquefasciatus* is particularly associated with various vector-spread diseases in several regions. Larvicides are insecticides designed to kill insects during their larval stage. Methoprene is an insect growth controller that prevents larvae from developing significantly beyond the pupa stage by interrupting their growth period. Methoprene is mildly toxic to a variety of crabs, shrimp, lobster, and crayfish and is extremely toxic to a variety of fish and aquatic herbivores; it tends to accumulate in fish tissues¹⁹. Olfaction plays an important role in many species and is linked to host-seeking, replication, predator recognition, and food detection²⁰. Odorant-binding proteins (OBPs) aid signal transduction by transporting odorants to olfactory receptors^{21,22}. Some example, consider previous reports, the ligand (5R,6S)-6-acetoxy-5-hexadecanolide^{23–25} was bound to OBP of the *C. quinquefasciatus* mosquito (PDB ID: 3OGN), it is best model for selection 1,5-diphenyl pent-4-en-1-one targets and molecular docking in this study.

The control of mosquitoes presents a substantial challenge, and currently inhibitors such as permethrin²⁶, organophosphates²⁷, fenthion^{28,29}, chlorpyrifos^{30–32}, temephos^{33,34}, diflubenzuron³⁵ and methoprene³⁶ are used; Fig. 1 details the compositions of these commercial insecticides. However, the use of chemical insecticides pose bigger challenges and various potential environmental problems, such as the widespread development of resistance and disruption of natural biological control systems^{37,38}. These problems require overcoming new mosquito larvae inhibitors and improving green methodologies, which can be achieved through Mannich base condensation reactions.



Scheme 1. Synthetic route of Mannich base derivative.

Mannich base synthesis is one of the best tools for green synthesis, in this way preparation of target compound based on cinnamylacetophenone (1,5-diphenylpent-4-en-1-one) comparable to cinnamylphenone (1,3-diphenylprop-2-en-1-one) (or) chalcone, Fig. 1, basically chalcone derivatives have mosquito larvicidal properties³⁹. Some publications have investigated the environmental study of chalcones⁴⁰ and 1,5-diphenylpent-4-en-1-one (cinnamylacetophenone)⁴¹. In general, chemical insecticides are the main agents used to reduce populations of vector mosquitoes⁴², even though their accessibility and use are limited by their toxicity to the environment and non-target organisms^{43,44} as well as the resistance of some mosquito species to them.

Chemically modified chalcones have been recently used to control insect populations; for instance, chalcone derivatives are toxic to *Ae. aegypti* first instar larvae and adults⁴⁵ and *Aedes albopictus* larvae⁴⁶. Some furan-chalcones are toxic to *Culex quinquefasciatus* larvae in the fourth stage of development⁴⁷.

The current work was focused on the presence of alkenyl imine/ β -amino ketones, particularly imines, which are frequently used in organic synthesis because of their high reactivity and the synthetic utility of the ensuing products⁴⁸. Furthermore, β -amino ketones and their analogues have shown effective medicinal properties^{49,50}. So that, current study was to determine novel water-soluble and nontoxic Mannich base 1,5-diphenylpent-4-en-1-one derivatives via grindstone green chemistry methodology that can be used to inhibit the second instar *Culex* mosquito larvae as a bio-indicator of aquatic pollution.

Results and discussion

Chemistry. A one-pot multicomponent synthesis of the title compounds was achieved using the grindstone green chemistry method. A mixture of acetophenone, cinnamaldehyde, substituted amine, and a catalytic amount of Cu(II)-tyrosinase enzyme was ground together in a pestle mortar. This was then followed by purification via column chromatography, in order to obtain the title compounds (**1a–1q**). The synthetic route outline is shown in Scheme 1. The chemical structures of synthesized compounds (**1a–1q**) were represented in Fig. 2. The active site in hydrolases is often thought to be responsible for promiscuous catalysis⁵¹. We suggest a mechanism for the Cu(II)-tyrosinase-catalysed Mannich reaction, outlined in Scheme 2, by combining this perspective with our findings, as mentioned above. First, the aldehyde and amine can easily react to form the Schiff base, and the ketone is simultaneously pre-activated by Cu(II)-tyrosinase to produce the enolate anion. Second, with the aid of the His residue of Cu(II)-tyrosinase, the Schiff base may form an intermediate complex. The Mannich adduct is then freed from the oxyanion hole after a proton is moved from the Schiff base to the enolate anion to create a new carbon–carbon bond. The core steps in this enzymatic mechanism are the formation of the enolate anion and the intermediate complex. Copper-containing materials such as coppertriflate⁵², copperacetate⁵³, copperbromide⁵⁴, and copper nanoparticles⁵⁵ play a vital role in Mannich base reactions. The one-pot multicomponent Mannich reaction was catalysed via various enzymes, such as trypsin⁵⁶, lipase⁵⁷, and protease⁵⁸. In the present study, copper containing the Cu(II)-tyrosinase enzyme was used as a catalyst for the synthesis of *N*-Mannich base (**1a–1q**) derivatives.

Some of the previously reported compounds, such as compound **1l**, were reported by β -acetamido ketones from cinnamaldehyde to react with acetophenone at room temperature, with L-proline used as a catalyst, to result in a yield of 75%. Another method was reported previously where *N*-substituted β -amino ketone derivatives had been produced by a one-pot multi-component process using copper(II)-phthalocyanine as a catalyst to result in an yield of 51%, which is comparable to the compound produced in the present work, which showed an 84% yield. Compound **1m** was also reported previously; an imine derived from an α,β -unsaturated aldehyde was also related to the present high binaphthol-derived monophosphoric acids as organocatalysts for enantioselective carbon–carbon bond-forming reactions, thus resulting in a product yield of 81%; an 82% yield was obtained in this study. There is no enzymatic catalysis was involved in the synthesis of compounds **1l** and **1m** in the literature. In our study we utilized Cu(II)-tyrosinase as a catalyst for producing compounds **1l** and **1m** and also the compounds acquired with high yields comparing previous literatures.

The compound **1a** was synthesised using the catalysts trypsin, lipase, protease, CuCl₂·2H₂O, and Cu(II)-tyrosinase with yields of 64%, 72%, 68%, 84%, and 92%, respectively. The use of the Cu(II)-tyrosinase enzyme green catalyst, instead of CuCl₂·2H₂O, increased the yield of the Mannich derivatives to 92% and reduced the reaction time. The optimisation of the reaction conditions and catalysts is presented in Table 1. The obtained compounds were analysed via FT-IR, ¹H, and ¹³C NMR spectroscopy. The key assignments of the compounds showed significant bands at 3170.23–3176.54, 2595.45–2599.98, and 1710.68–1716.70 cm⁻¹ in the IR spectrum, conforming to the –NH, –C=N, and –C=O groups, respectively. The ¹H NMR showed signals at δ 8.03–9.70, 3.82–4.81 and 2.40–2.98 ppm, indicating –NH, 4-CH, and –CH₂ protons, respectively. The ¹³C NMR showed

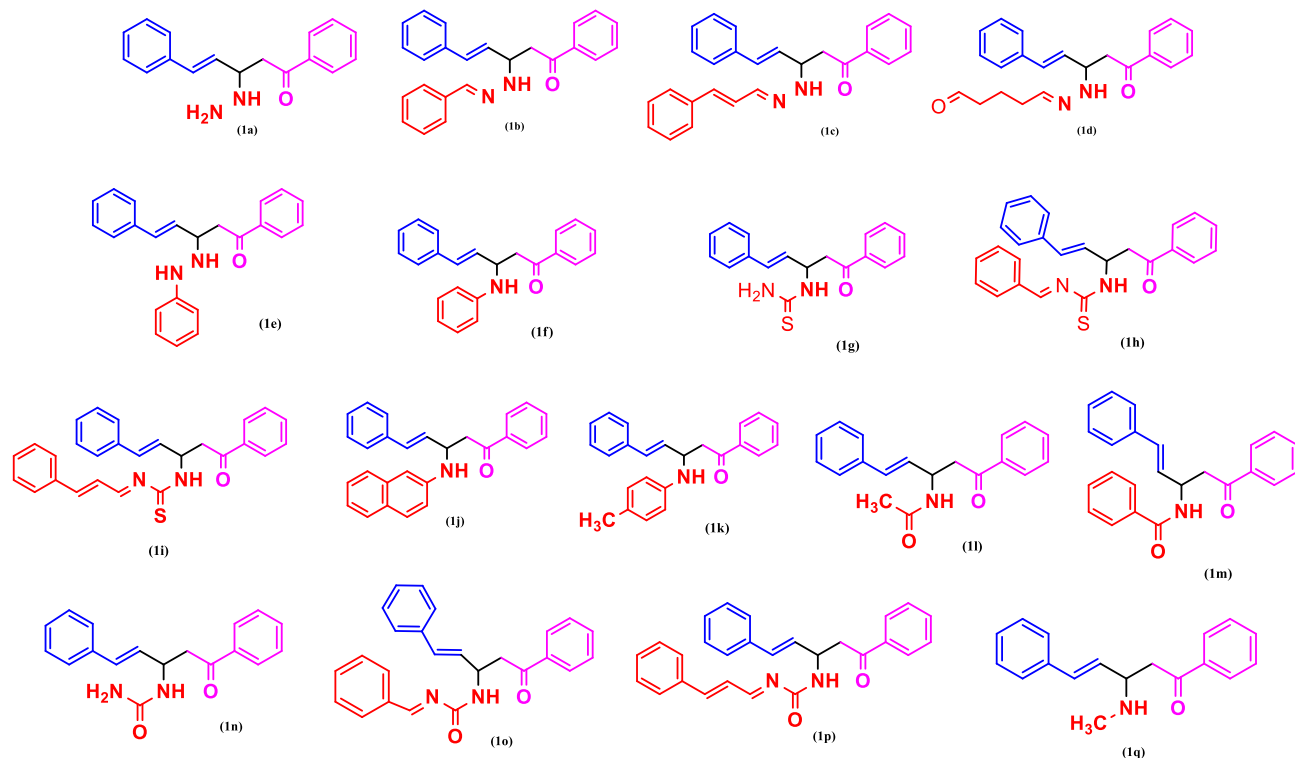


Figure 2. Structures of synthesized Mannich base derivatives (**1a–1q**) drawn by ChemDraw Ultra 12.0 Suite (PerkinElmer, USA).

peaks at δ 197.4–197.6, 48.4–59.2, and 48.0–50.6 ppm, which conforms to $-\text{C}=\text{O}$, $-\text{CH}$, and $-\text{CH}_2$ atoms, respectively. Mass spectra and elemental analysis were used to determine the conformation of all these compounds.

“In general, *E*-alkenyl imines are organized from the corresponding *E*-alkenyl aldehydes through imine precursors^{59–61}. In this reaction, the carbon–carbon bond formation rate allows the isomerisation of the in situ generated *E*-alkenyl imine from *E*-alkenyl aldehydes with secondary amine and acetophenone, in the presence of 5 mol% of Cu(II)-tyrosinase catalysis to afford the corresponding Mannich adducts (**1a–1q**) in moderate to good yields with high *E*-selectivity”.

NOE NMR data (see Supplementary Material) clearly confirmed the stereochemistry of the *E* isomers of compounds **1a**, and **1i**. Thus, based on this study the spectroscopic characteristic downfield shift is observed for this pent-4-en-1-one proton in the *E*-isomer than in the *Z*-isomer.

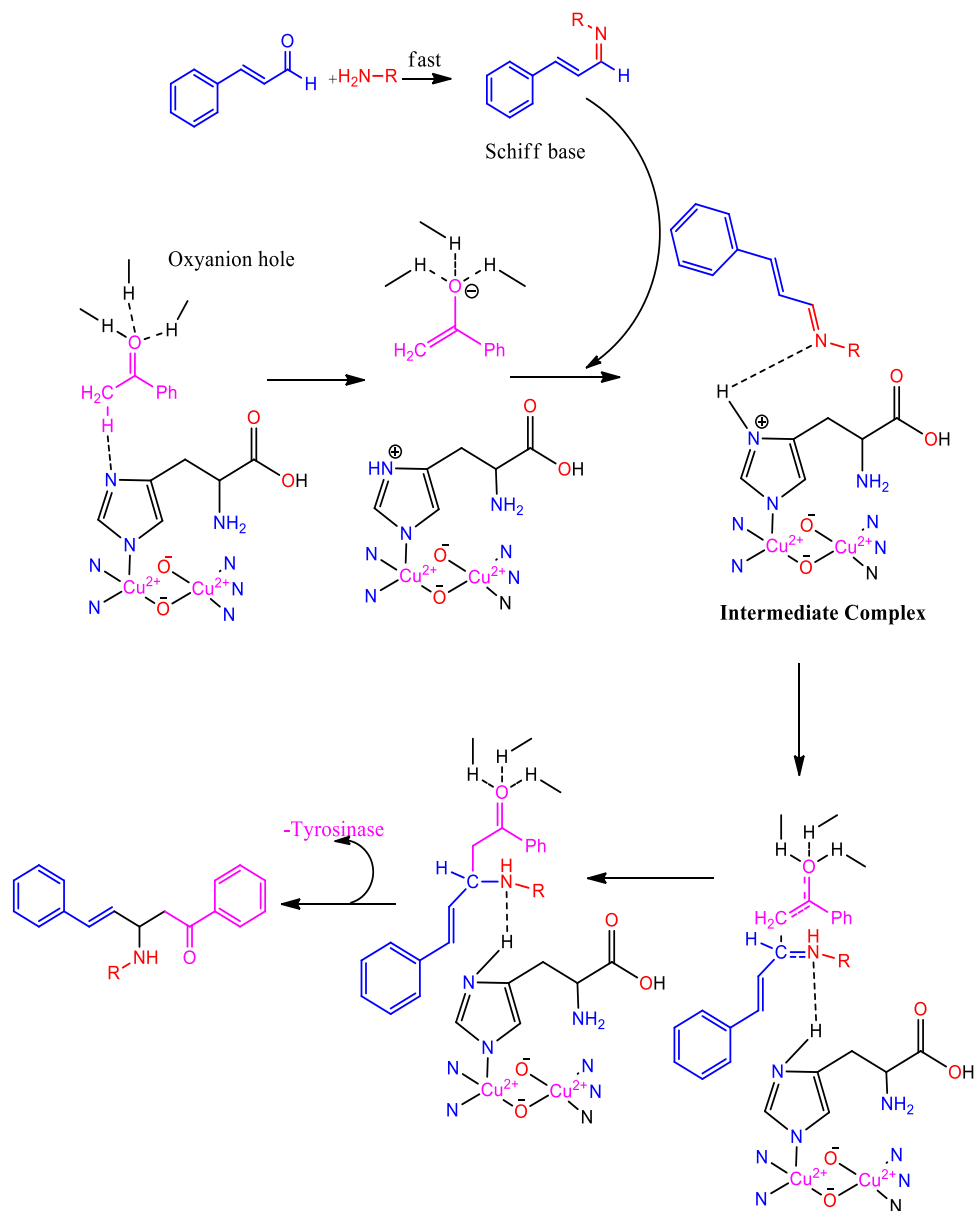
Catalyst recovery studies. The recovered catalyst was recycled for at least 10 run times with a small defeat in catalytic action (Fig. 3). The decrease in catalytic action perceived through the reinforced catalyst on recycling might be owing to limited loss of basic locates or loss of catalyst surface area during regeneration/reaction. The values are displayed in Table 2.

Biological activity. A total of 17 compounds (**1a–1q**) were tested against second instar *C. quinquefasciatus* larvae, and the toxicity of the title compounds was assessed in the marine fish *Oreochromis mossambicus*. Toxicity was defined as the ratio of deaths (%) at 24 h. Structure–activity relationships showed that the final compounds contained 1,5-diphenylpent-4-en-1-one with different types of amines, thus exerting larvicidal and toxic effects based on the formation of the specific chemical composition.

Compound **1i** showed a higher larvicidal activity than other compounds, with an LD_{50} of 28.5 μM , which was better than that of the controls temephos (LD_{50} of 37.9 μM)⁶² and permethrin (LD_{50} of 54.6 μM). The antifeedant induced 0% mortality even at $\text{LD}_{50} > 100 \mu\text{M}$, which was represented by no toxicity in water.

Compound **1a** induced 80% mortality at 100 μM and its LD_{50} value was 223.0 μM , whereas the antifeedant induced 100% mortality at 100 μM and had a LD_{50} value of 49.5 μM . This suggests that the presence of the hydrazine group may be the reason for the observed antifeedant-induced 100% mortality, as evident from toxicity against *O. mossambicus* fingerlings within 15 min of screening.

Compounds **1f** and **1j** induced a mortality rate of 80% with LD_{50} values of 177.4 μM and 154.9 μM , respectively, in larvicidal screening whereas they induced 100% mortality in antifeedant screening. This suggests that the presence of aniline and naphthalen-2-amine groups may be the reason for the observed biological effects, respectively.



Scheme 2. Proposed mechanism of Mannich base derivative formation.

Entry	Catalyst	Yield (%)	Time (min)
1	No enzyme	06	30
2	Trypsin from bovine pancreas	64	8
3	Lipase from <i>Candida antarctica</i>	72	12
4	Protease from <i>Streptomyces griseus</i>	68	10
5	$\text{CuCl}_2 \cdot 2\text{H}_2\text{O}$	84	5
6	Cu(II)-Tyrosinase from mushroom	92	2

Table 1. Catalyst optimization for compound **1a**.

Compounds **1m** and **1n** induced a mortality rate of 80% with LD_{50} values of 159.8 μM and 190.9 μM , respectively, in larvicidal screening whereas they induced 0% mortality in antifeedant screening. This suggests that the presence of the benzamide and urea groups could be the reason for the respective observed biological effects.

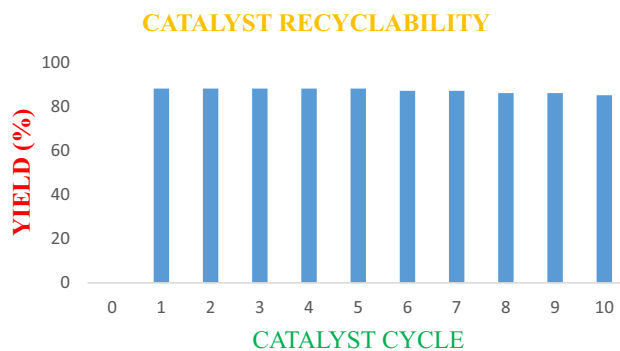


Figure 3. Catalyst recyclability activity of Cu(II)-tyrosinase enzyme drawn by Microfoft Office 2019 Suite.

Entry	Catalyst	Yield (%)
1	1st use	92
2	2nd use	92
3	3rd use	90
4	4th use	90
5	5th use	88
6	6th use	87
7	7th use	87
8	8th use	86
9	9th use	86
10	10th use	85

Table 2. Recyclability of Cu(II)-tyrosinase enzyme catalyst.

Compounds **1d** and **1o** induced 0% mortality at 100 μ M in both the larvicidal and antifeedant screening. This suggests that the presence of the 5-hydrazonepentanal and 1-benzylideneurea groups may be the reason for the observed biological effect as they exhibited no active or toxic behaviour.

The above analysis therefore indicates that compound **1i** was significantly active in larvicidal screening and displayed low toxicity in antifeedant screening. The percentages of mortality and LD₅₀ values are presented in Tables 3 and 4.

Culex quinquefasciatus larval growth regulation. To explore the impact of 1,5-diphenylpent-4-en-1-one formulations on *C. quinquefasciatus* larvae growth, metamorphosis, and production, we exposed the larvae to compound **1i** for 72 h. Table 5 summarizes the effects of compound **1i** impact on larval weight and growth inhibition. When subjected to 10 μ M of compound **1i**, the eclosion rate and time of the pupal and adult periods of administered *C. quinquefasciatus* is calculated, and the findings are seen in Table 6. Compound **1i** had a growth-inhibition score of 41.36% and suppressed larval weight development. Furthermore, compound **1i** had little effect on the duration of the adult and pupal periods, but it did result in a 55 percent eclosion rate. Compound **1i** hindered the production and growth of *C. quinquefasciatus* larvae, according to these findings.

Docking results. The Autodock Vina program was used to assess the docking behavior between compounds **1i**, **permethrin** and **temephos** with the mosquito odorant binding protein (PDB ID: 3OGN). Compound **1i** displayed more binding affinity (– 10.0 kcal/mol) than other compounds and **permethrin** (– 9.7 kcal/mol) and **temephos** (– 7.6 kcal/mol) with the mosquito odorant binding protein (PDB ID: 3OGN). Residues of the amino acids Leu19, Leu73, Leu76, His77, Ala78, Trp114, and Leu124 were tangled in hydrophobic connections. The interaction of compound **1i** with mosquito odorant binding protein (PDB ID: 3OGN) is shown in Fig. 4. In the control **permethrin**, residues of the amino acids Leu15, Leu19, Phe59, Leu73, Leu76, His77, Leu80, Ala88, Met89, Gly92, His111, Trp114, Phe123, and Leu124 were tangled in hydrophobic connections.

The positive control **permethrin** connected in the mosquito odorant binding protein (PDB ID: 3OGN) protein is shown in Fig. 5. The control **temephos** displayed three hydrogen bond interactions with the receptor mosquito odorant binding protein (PDB ID: 3OGN). The amino acid residue Ser79 showed two hydrogen bonds with **temephos**, with the bond lengths of 3.32 and 2.26 Å, and the amino acid residue Ala88 showed one hydrogen bond with **temephos**, with the bond length of 3.25 Å. Residues of the amino acids Leu19, Ala62, Leu76, Met91, Trp114, and Tyr122 were involved in hydrophobic contacts with the receptor. The interaction of the control **temephos** with the mosquito odorant binding protein (PDB ID: 3OGN) protein is shown in Fig. 6. The inhibitor representation of inhibitor molecule docked into the receptor was shown in Figs. 4a, 5a, and 6a. The inhibitor

Compounds	% of Mortality at 25 μM	% of Mortality at 50 μM	% of Mortality at 100 μM	LD ₅₀ (μM) ^a
1a	24.1 ± 0.2	43.2 ± 0.1	80.2 ± 0.2	223.0 ± 0.0
1b	11.2 ± 0.2	27.1 ± 0.2	40.1 ± 0.1	282.1 ± 0.0
1c	19.3 ± 0.4	26.3 ± 0.4	40.2 ± 0.6	262.8 ± 0.0
1d	0 ± 0.0	0 ± 0.0	0 ± 0.0	286.9 ± 0.0
1e	33.3 ± 0.1	48.3 ± 0.2	60.4 ± 0.2	193.3 ± 0.3
1f	25.0 ± 0.2	44.1 ± 0.2	80.0 ± 0.2	177.4 ± 0.2
1g	22.1 ± 0.2	34.2 ± 0.2	40.1 ± 0.3	322.1 ± 0.0
1h	34.5 ± 0.2	47.9 ± 0.3	60.1 ± 0.2	165.1 ± 0.2
1i	68.2 ± 0.4	88.2 ± 0.6	100 ± 0.0	28.5 ± 0.2
1j	26.1 ± 0.2	44.5 ± 0.2	80.4 ± 0.3	154.9 ± 0.2
1k	0 ± 0.0	0 ± 0.0	0 ± 0.0	292.8 ± 0.0
1l	20.8 ± 0.1	20.8 ± 0.1	20.8 ± 0.1	340.8 ± 0.0
1m	29.9 ± 0.3	42.3 ± 0.3	80.9 ± 0.3	159.8 ± 0.2
1n	29.9 ± 0.2	43.6 ± 0.2	81.0 ± 0.2	190.9 ± 0.0
1o	0 ± 0.0	0 ± 0.0	0 ± 0.0	261.4 ± 0.0
1p	40.4 ± 0.1	40.4 ± 0.1	40.4 ± 0.1	244.8 ± 0.0
1q	20.4 ± 0.2	20.4 ± 0.2	20.4 ± 0.2	376.8 ± 0.0
Permethrin	51.1 ± 1.0	76.3 ± 0.1	100 ± 0.0	54.6 ± 0.0
Temephos	56.1 ± 0.2	79.3 ± 0.2	100 ± 0.0	37.9 ± 0.0

Table 3. Larvicidal activity of compounds (**1a–1q**). Larvicidal activity model is used for the activity assays (second instar *C. quinquefasciatus*), one-day-old larvae were considered as 2nd instar. ^aValues are mean ± SD (n = 3). Lethal Dose (LD₅₀): the LD₅₀ is one way to measure the short-term poisoning potential (acute toxicity) of a material.

Compounds	% of Mortality at 10 μM	% of Mortality at 25 μM	% of Mortality at 50 μM	% of Mortality at 100 μM	LD ₅₀ (μM) ^a
1a	33.3 ± 0.2	66.2 ± 0.0	88.2 ± 0.0	100 ± 0.0	49.5 ± 0.7
1b	20.2 ± 0.3	20.2 ± 0.3	20.2 ± 0.3	20.2 ± 0.3	282.1 ± 0.0
1c	0 ± 0.0	0 ± 0.0	0 ± 0.0	0 ± 0.0	262.8 ± 0.0
1d	0 ± 0.0	0 ± 0.0	0 ± 0.0	0 ± 0.0	286.9 ± 0.0
1e	31.3 ± 0.0	66.1 ± 0.0	82.2 ± 0.0	100 ± 0.0	47.8 ± 0.0
1f	41.2 ± 0.0	51.3 ± 0.0	72.2 ± 0.0	100 ± 0.0	64.4 ± 0.4
1g	–	5.2 ± 0.1	10.3 ± 0.1	20.6 ± 0.2	322.1 ± 0.0
1h	5.3 ± 0.1	20.2 ± 0.1	49.4 ± 0.1	60.4 ± 0.1	131.2 ± 0.8
1i	0 ± 0.0	0 ± 0.0	0 ± 0.0	0 ± 0.0	235.5 ± 0.0
1j	42.2 ± 0.4	59.2 ± 0.3	88.2 ± 0.0	100 ± 0.0	26.7 ± 0.2
1k	33.1 ± 0.0	67.1 ± 0.74	87.9 ± 0.0	100 ± 0.0	40.4 ± 0.6
1l	–	5.2 ± 0.1	10.3 ± 0.1	20.2 ± 0.1	340.8 ± 0.0
1m	0 ± 0.0	0 ± 0.0	0 ± 0.0	0 ± 0.0	281.3 ± 0.0
1n	0 ± 0.0	0 ± 0.0	0 ± 0.0	0 ± 0.0	339.7 ± 0.0
1o	0 ± 0.0	0 ± 0.0	0 ± 0.0	0 ± 0.0	261.4 ± 0.0
1p	0 ± 0.0	0 ± 0.0	0 ± 0.0	0 ± 0.0	244.8 ± 0.0
1q	–	5.2 ± 0.1	10.3 ± 0.1	20.2 ± 1.0	376.8 ± 0.0

Table 4. Antifeedant activity of compounds (**1a–1q**). Antifeedant activity for the toxicity measurement against marine fish *Oreochromis*. ^aValues are mean ± SD (n = 3). The LD₅₀ is one way to measure the short-term poisoning potential (acute toxicity) of a material.

Compound	Weight of larvae (mg)		Weight gain (mg)	Inhibition (%)
	0 h	72 h		
1i^a	100.3 ± 1.9	104.1 ± 0.2	3.9 ± 0.9	41.4 ± 2.8
Control^b	100.16 ± 0.3	106.7 ± 1.5	6.6 ± 1.4	–

Table 5. Compound **1i** on the growth of *Culex quinquefasciatus*. ^aThe concentration of 1i was 10 μM . ^bControl is not containing the compounds.

Compound	Duration of pupae (h)	Duration of adult (h)	Rate of eclosion (%)
1i ^a	68.1 ± 0.64	23.1 ± 1.36	55 ± 1.7
Control ^b	65.5 ± 1.21	24.2 ± 0.82	80 ± 1.0

Table 6. Analysis of progress of *Culex quinquefasciatus* growth. ^aThe concentration of **1i** was 10 μM. ^bControl is not containing the compounds.

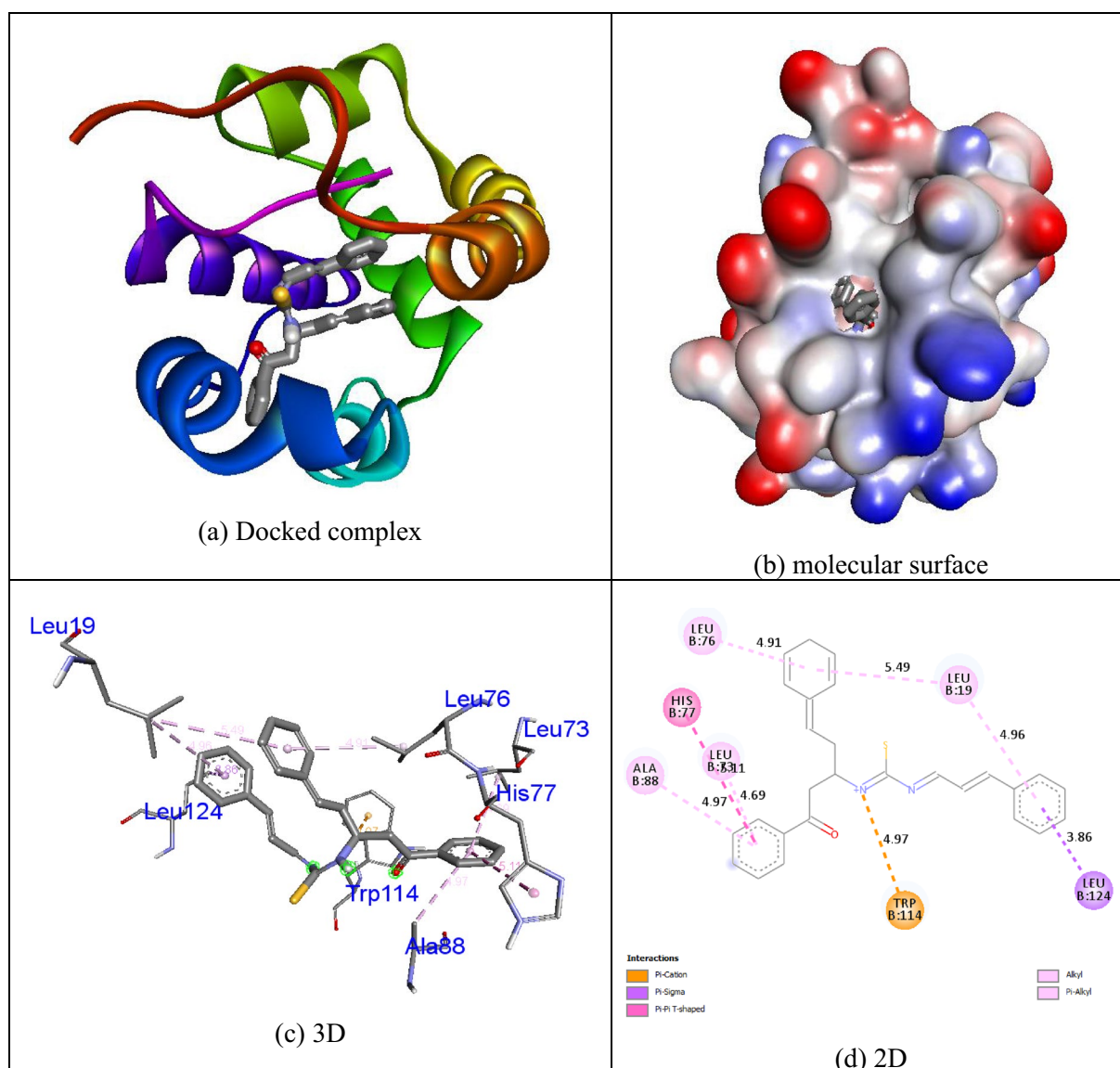


Figure 4. Molecular docking representation of ligand **1i** within the active site of mosquito odorant binding protein (PDB ID: 3OGN). Chemical structures were drawn by ChemDraw Ultra 12.0 Suite (PerkinElmer, USA) and analyzed by the Discovery studio visualizer (BIOVIA Discovery studio 2019 Client).

molecule docked into the binding pocket of the receptor was shown in Figs. 4b, 5b, and 6b. The 3D representation of inhibitor molecule docked into the receptor was shown in Figs. 4c, 5c, and 6c. The 2D representation molecule docked with receptor was shown in Figs. 4d, 5d, and 6d. The results show that compound **1i** possesses comparable inhibition abilities relative to the controls **permethrin** and **temephos**. The results are listed in Table 7.

MD simulation analysis. The protein–ligand complex structure of ligand **1i** with 3OGN stability was carried out by Molecular Dynamics (MD) simulation method using Gromacs. Root Mean Square Deviation (RMSD) plot is an important to know the stability of the complex structure. From the analysis of values of RMSD plot, the values from 4.5 to 10 ns shows that the structure was stable because Ca backbone of protein was not fluctuated more (Fig. 7).

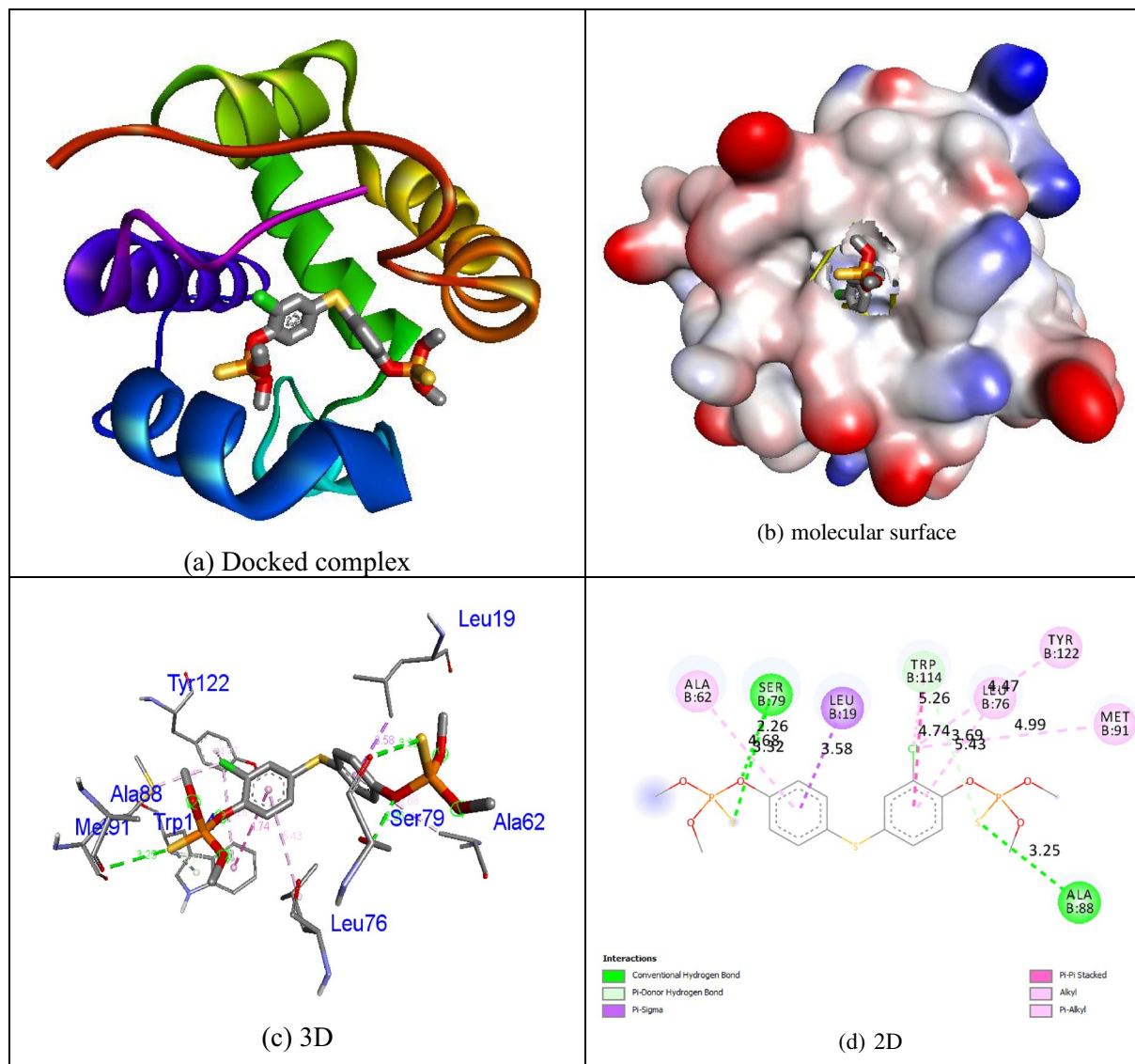


Figure 6. Molecular docking representation of ligand **temephos** within the active site of mosquito odorant binding protein (PDB ID: 3OGN). Chemical structures were drawn by ChemDraw Ultra 12.0 Suite (PerkinElmer, USA) and analyzed by the Discovery studio visualizer (BIOVIA Discovery studio 2019 Client).

General procedure for the synthesis of compounds (1a–1q). A reaction mixture made up of cinnamaldehyde (0.01 mol, 1.32 mL), acetophenone (0.01 mol, 1.20 mL), substituted amine (0.01 mol) and Cu(II)-tyrosinase enzyme (0.5 g) was mixed in a mortar and ground at RT. Then 2 mL of 50 mM potassium phosphate buffer (pH 6.0) was added and filtered to recover the catalyst. The final filtered solid material was separated using column chromatography (Ethyl acetate:hexane6). The same method was followed when mixing compounds **1b–1q**.

3-Hydrazinyl-1,5-diphenylpent-4-en-1-one (1a). White solid; mp: 110–112 °C; Yield: 92%; Water solubility: 0.11 mM/mL; IR(KBr) ν : 3171.48, 3065.51, 3041.02, 1715.02, 1624.53 cm^{-1} ; ^1H NMR (300 MHz): δ 9.20 (s, 1H), 8.84 (s, 2H, NH_2), 7.97–7.96 (dd, $J=7.33$ Hz, $J=7.37$ Hz, 2H, Ar-ring), 7.63–7.60 (d, $J=6.21$ Hz, 1H, Ar-ring), 7.53–7.51 (dd, $J=7.30$ Hz, $J=7.34$ Hz, 2H, Ar-ring), 7.41–7.37 (dd, $J=7.33$ Hz, $J=7.37$ Hz, 2H, Ar-ring), 7.34 (d, $J=6.22$ Hz, 1H, Ar-ring), 7.21 (dd, $J=7.30$ Hz, $J=7.35$ Hz, 2H, Ar-ring), 6.56–6.51 (d, $J=6.22$ Hz, 1H, CH), 6.19–6.14 (d, $J=6.22$ Hz, 1H), 3.84–3.80 (m, 1H), 2.94–2.91 (d, $J=6.21$ Hz, 2H); ^{13}C NMR (75 MHz): 197.4 (1C), 136.7, 133.1, 128.8, 128.6 (6C, Ph ring), 136.4, 128.6, 128.5, 127.9 (6C, Ar ring), 133.4 (1C), 128.4 (1C), 59.2 (1C), 48.0 (1C); EIMS (m/z): 267.15 (M^+ , 18%); Anal. Calcd. for $\text{C}_{17}\text{H}_{18}\text{N}_2\text{O}$: C, 76.66; H, 6.81; N, 10.52%; found: C, 76.68; H, 6.80; N, 10.51%.

3-(2-Benzylidenehydrazinyl)-1,5-diphenylpent-4-en-1-one (1b). Greenish solid; mp: 145–148 °C; Yield: 86%; Water solubility: 0.06 mM/mL; IR(KBr) ν : 3176.51 (NH), 3072.50, 3032.32, 2596.43, 1716.08, 1623.43;

Compounds	Mosquito odorant-binding protein 3OGN		
	Binding affinity (kcal/mol)	No. of H-bonds	H-bonding residues
1a	− 9.0	2	His121, Phe123
1b	− 9.7	0	−
1c	− 9.0	0	−
1d	− 8.8	0	−
1e	− 9.7	1	Phe123
1f	− 9.6	0	−
1g	− 8.3	0	−
1h	− 9.3	0	−
1i	− 10.0	0	−
1j	− 9.8	0	−
1k	− 9.8	0	−
1l	− 8.9	0	−
1m	− 9.8	0	−
1n	− 8.8	0	−
1o	− 9.5	0	−
1p	− 9.2	0	−
1q	− 8.3	0	−
Temephos	− 7.6	3	Ser79, Ala88
Permethrin	− 9.7	0	−

Table 7. Molecular docking interaction of compounds (**1a–1q**) and control Temephos, Permethrin.

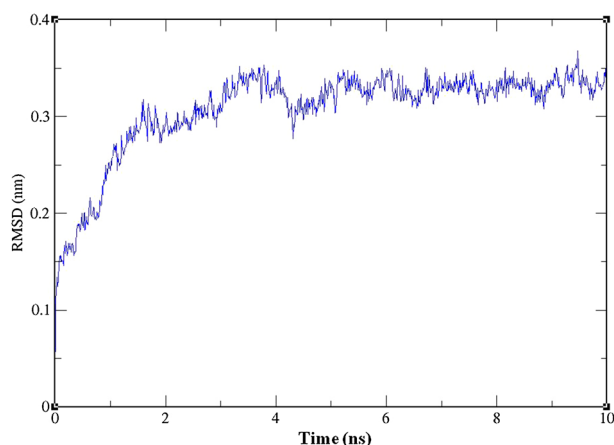


Figure 7. Graphical representation of Time vs. RMSD map for Protein after ligand fit to the protein during molecular dynamics simulation. XMGrace (Version 5.1.19) tool was used to prepare the graphs (Turner, Land-Margin Research, & Technology, 2005).

^1H NMR(300 MHz): δ 9.21(s,1H), 8.36(s,1H,-CH), 7.97–9.94(dd, $J=7.33$ Hz, $J=7.37$ Hz), 7.86–7.81 (dd, $J=7.33$ Hz, $J=7.37$ Hz), 7.63–7.60(d, $J=6.21$ Hz, 1H, Ph), 7.55–7.53(dd, $J=7.31$ Hz, $J=7.34$ Hz, 2H), 7.50–7.47(m, 3H, Ar ring), 7.40–7.38(dd, $J=7.33$ Hz, $J=7.37$ Hz, 2H, Ar ring), 7.34–7.31(d, $J=6.21$ Hz, 1H, Ar ring), 7.20–7.17(dd, $J=7.31$ Hz, $J=7.35$ Hz, 2H, Ar ring), 6.58–6.54 (d, 1H, $J=6.21$ Hz, CH), 6.18–6.14(d, $J=6.21$ Hz, 1H, CH), 3.80–3.76(m, 1H, CH), 2.95–2.92(d, $J=6.21$ Hz, 2H, CH_2); ^{13}C NMR (75 MHz): 197.6 (1C), 143.3 (1C), 136.6, 133.0, 128.7, 128.5(6C, Ph ring), 136.5, 128.7, 128.6, 128.0(6C, Ar ring), 134.4(1C), 133.7, 131.0, 129.2, 128.8 (6C, Ph ring), 128.5(1C), 55.1(1C), 48.5(1C); EIMS(m/z) 355.18 (M^+ , 26%); Anal. Calcd. for $\text{C}_{24}\text{H}_{22}\text{N}_2\text{O}$: C, 81.33; H, 6.26; N, 7.90%; found: C, 81.31; H, 6.27; N, 7.91%.

1,5-Diphenyl-3-(2-(3-phenylallylidene)hydrazinyl)pent-4-en-1-one (1c). Light green powder; mp: 148–150 °C; Yield: 88%; Water solubility: 0.14 mM/mL; IR(KBr) ν 3176.50, 3073.51, 3031.30, 2595.45, 1714.08, 1624.40 cm^{-1} ; ^1H NMR(300 MHz): δ 9.26(s, 1H, NH), 7.95–7.91(dd, $J=7.33$ Hz, $J=7.37$ Hz), 7.63–7.60–7.58(d, $J=6.21$ Hz, 1H), 7.57–7.54(dd, $J=7.33$ Hz, $J=7.37$ Hz, 2H), 7.53–7.50(dd, $J=7.31$ Hz, $J=7.35$ Hz, 2H, Ph), 7.50(s, 1H, CH), 7.40–7.37(dd, $J=7.33$ Hz, $J=7.37$ Hz, 4H, Ar ring), 7.36–7.33 (d, $J=6.21$ Hz, 2H, Ar-ring), 7.24–7.21(dd, $J=7.31$ Hz, $J=7.35$ Hz, 2H, Ar ring), 6.54–6.52(d, $J=6.21$ Hz, 2H, CH), 6.17–6.12(d, $J=6.21$ Hz, 2H, CH),

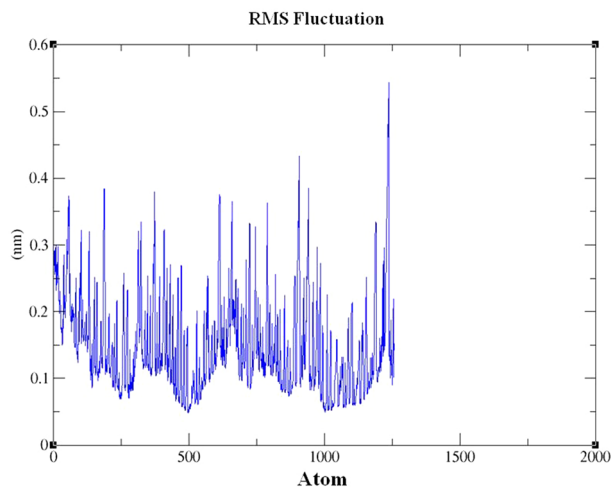


Figure 8. Graphical representation of RMS Fluctuation map during molecular dynamics simulation. XMgrace (Version 5.1.19) tool was used to prepare the graphs (Turner, Land-Margin Research, & Technology, 2005).

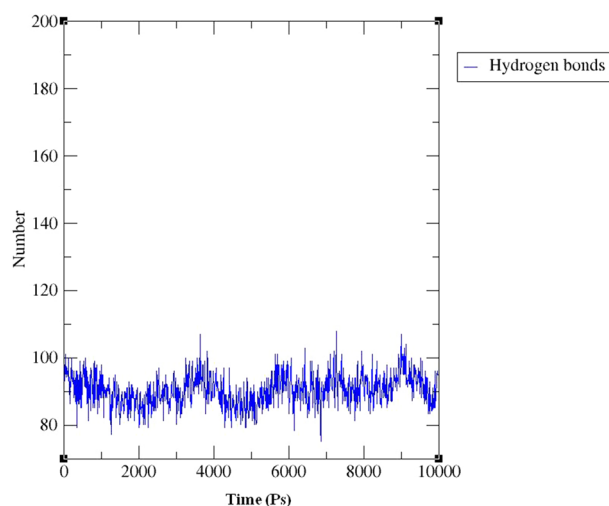


Figure 9. The hydrogen bond interaction between the protein 3OGN and compound 1i. XMgrace (Version 5.1.19) tool was used to prepare the graphs (Turner, Land-Margin Research, & Technology, 2005).

3.78–3.74(m, 1H), 2.92–2.89 (d, $J=6.21$ Hz, 2H); ^{13}C NMR (75 MHz): 197.2 (1C), 137.2 (1C), 136.7, 133.1, 128.8, 128.6, (6C, Ph ring), 136.4, 128.6, 128.5, 127.8 (6C, Ar ring), 135.2, 128.6, 128.5, 127.9(6C, Ph ring), 133.9, 133.7, 128.2, 125.3, 56.2, 48.5; EIMS(m/z): 381.19(M^+ , 28%); Anal. Calcd. for $\text{C}_{26}\text{H}_{24}\text{N}_2\text{O}$: C, 82.07; H, 6.36; N, 7.36%; found: C, 82.05; H, 6.37; N, 7.37%.

5-(2-(5-Oxo-1,5-diphenylpent-1-en-3-yl)hydrazono)pentanal (1d). White powder; mp: 126–129 °C; Yield: 85%; Water solubility: 0.08 mM/mL; IR(KBr) ν : 3176.54, 3073.50, 3031.32, 2595.48, 1714.18, 1624.45; ^1H NMR (300 MHz): δ 9.70(s, 1H, CH), 9.24(s, 1H), 7.97–7.94(dd, $J=7.33$ Hz, $J=7.37$ Hz, 2H), 7.60–7.57(d, $J=6.21$ Hz, 1H), 7.53–7.50(dd, $J=7.31$ Hz, $J=7.33$ Hz, 2H), 7.42–7.37(dd, $J=7.33$ Hz, $J=7.37$ Hz, 2H, Ar ring), 7.34–7.31(d, $J=6.21$ Hz, 1H, Ar ring), 7.21(dd, $J=7.31$ Hz, $J=7.35$ Hz, 2H, Ar ring), 6.97(s, 1H, CH), 6.56–6.51(d, $J=6.21$ Hz, 1H), 6.16–6.13(1H, d, $J=6.21$ Hz, CH), 3.85–3.82(m, 1H, CH), 2.93–2.88 (d, $J=6.21$ Hz, 2H), 2.42–2.36(m, 2H), 1.82–1.74(m, 2H), 1.53–1.49 (m, 2H); ^{13}C NMR(75 MHz): 202.2, 197.4, 158.3, 136.7, 133.1, 128.8, 128.6, (6C, Ph ring), 136.4, 128.6, 28.5, 127.9(6C, Ar ring), 134.7, 134.1, 127.9, 56.1, 48.5, 43.3, 25.9(1C); EIMS(m/z): 349.19(M^+ , 24%); Anal. Calcd. for $\text{C}_{22}\text{H}_{24}\text{N}_2\text{O}_2$: C, 75.83; H, 6.94; N, 8.04%; found: C, 75.80; H, 6.96; N, 8.06%.

1,5-Diphenyl-3-(2-phenylhydrazinyl)pent-4-en-1-one (1e). White powder; mp: 143–145 °C; Yield: 88%; Water solubility: 0.20 mM/mL; IR(KBr) ν : 3176.52, 3073.50, 3031.28, 1714.10, 1624.38 cm^{-1} ; ^1H NMR(300 MHz): δ 9.22 (s, 1H), 9.16(s, 1H), 7.97(dd, $J=7.34$ Hz, $J=7.38$ Hz, 2H, Ph), 7.65(d, $J=6.21$ Hz, 1H), 7.55–7.53(dd,

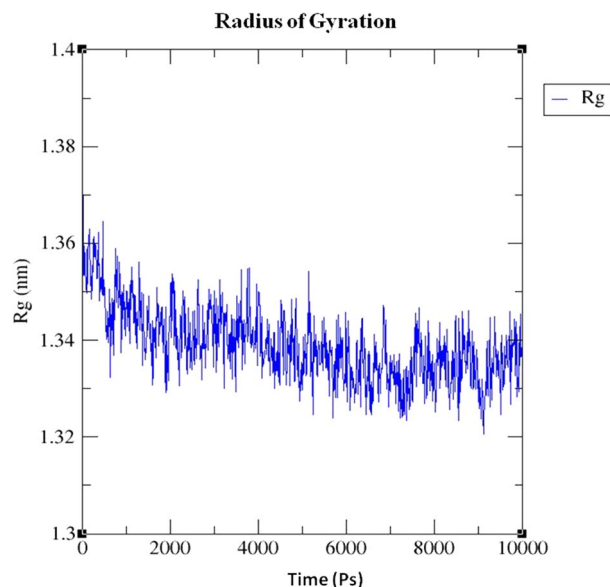


Figure 10. Radius of gyration value of complex structure of protein 3OGN bounded with the compound **1i**. XMGrace (Version 5.1. 19) tool was used to prepare the graphs (Turner, Land-Margin Research, & Technology, 2005).

$J=7.31$ Hz, $J=7.35$ Hz, 2H), 7.38–7.34(dd, $J=7.33$ Hz, $J=7.37$ Hz, 2H, Ar ring), 7.35–7.32(dd, $J=7.31$ Hz, $J=7.35$ Hz, Ph), 7.32–7.30(d, $J=6.21$ Hz, 1H, Ar-ring), 7.21–7.19(dd, $J=7.31$ Hz, $J=7.35$ Hz, 2H, Ar-ring), 7.02–6.98(dd, $J=7.31$ Hz, $J=7.35$ Hz, 2H, Ph), 6.88–6.86 (d, $J=6.21$ Hz, 1H, Ar-ring), 6.56–6.54(d, $J=6.22$ Hz, 1H), 6.17–6.15(d, $J=6.21$ Hz, 1H), 3.84–3.79(m, 1H), 2.95–2.92(d, $J=6.21$ Hz, 2H); ^{13}C NMR (75 MHz): 197.4(1C), 136.7, 133.1, 128.8, 128.6, (6C, Ph ring), 136.4, 128.6, 128.5, 127.8 (6C, Ar ring), 151.0, 129.2, 122.8, 113.2 (6C, Ph ring), 134.2, 127.9, 56.6, 48.3; EIMS(m/z): 343.18 (M^+ , 25%); Anal. Calcd. for $\text{C}_{23}\text{H}_{22}\text{N}_2\text{O}$: C, 80.67; H, 6.48; N, 8.18%; found: C, 80.65; H, 6.47; N, 8.19%.

1,5-Diphenyl-3-(phenylamino)pent-4-en-1-one (1f). Yellow powder; mp: 101–103 °C; Yield: 86%; Water solubility: 0.16 mM/mL; IR(KBr) ν : 3176.53, 3072.50, 3030.28, 1715.10, 1623.38; ^1H NMR (300 MHz): δ 9.26(s, 1H, NH), 7.97–7.95(dd, $J=7.33$ Hz, $J=7.37$ Hz, 2H), 7.67–7.63(d, $J=6.21$ Hz, 1H), 7.53–7.51(dd, $J=7.31$ Hz, $J=7.35$ Hz, 2H), 7.44–7.41(dd, $J=7.33$ Hz, $J=7.37$ Hz, 2H, Ar ring), 7.35–7.30 (d, $J=6.21$ Hz, 1H, Ar-ring), 7.28–7.23(dd, $J=7.31$ Hz, $J=7.35$ Hz, 2H, Ar-ring), 7.25–7.19(dd, $J=7.31$ Hz, $J=7.35$ Hz, 2H, Ph), 6.83–6.80(dd, $J=7.31$ Hz, $J=7.35$ Hz, 2H, Ph), 6.74–6.71(d, $J=6.21$ Hz, 1H, Ar ring), 6.56–6.54 (d, $J=6.20$ Hz, 1H, CH), 6.19–6.17(d, $J=6.21$ Hz, 1H), 3.84–3.79(m, 1H, -CH), 2.90–2.87(d, $J=6.21$ Hz); ^{13}C NMR (75 MHz): 197.4(1C), 136.7, 133.1, 128.8, 128.6, (6C, Ph ring), 136.4, 128.6, 128.5, 127.9 (6C, Ar ring), 147.6, 129.5, 120.8, 119.7 (6C, Ph ring), 133.1, 127.7, 57.2, 50.5; EIMS(m/z): 328.17 (M^+ , 25%); Anal. Calcd. for $\text{C}_{23}\text{H}_{21}\text{NO}$: C, 84.37; H, 6.46; N, 4.28%; found: C, 84.30; H, 6.49; N, 4.30%.

1-(5-Oxo-1,5-diphenylpent-1-en-3-yl)thiourea (1g). Green solid; mp: 139–141 °C; Yield: 91%; Water solubility: 0.24 mM/mL; IR(KBr) ν : 3176.51, 3072.74, 3029.32, 1712.18, 1625.45; ^1H NMR (300 MHz): δ 9.22(1H, s, NH), 8.52(s, 2H, NH_2), 7.97–7.94(dd, $J=7.33$ Hz, $J=7.37$ Hz, 2H), 7.63–7.61(d, $J=6.21$ Hz, 1H, Ph), 7.55–7.50(dd, $J=7.31$ Hz, $J=7.35$ Hz, 2H, Ph), 7.40–7.36(dd, $J=7.33$ Hz, $J=7.37$ Hz, 2H, Ar ring), 7.33–7.30(1H, d, $J=6.21$ Hz, Ar ring), 7.23–7.19(dd, 2H, $J=7.31$ Hz, $J=7.35$ Hz, Ar ring), 6.56–6.54(d, $J=6.22$ Hz, 1H), 6.19–6.17(d, $J=6.21$ Hz, 1H), 3.82–3.79(m, 1H), 2.98–2.96 (d, $J=6.20$ Hz, 2H); ^{13}C NMR (75 MHz): 197.4(1C), 182.0(1C), 136.7, 133.1, 128.8, 128.6, (6C, Ph ring), 136.4, 128.6, 28.5, 127.9 (6C, Ar ring), 134.2, 128.2, 55.6, 50.6; EIMS(m/z) 311.12 (M^+ , 19%); Anal. Calcd. for $\text{C}_{18}\text{H}_{18}\text{N}_2\text{S}\text{O}$: C, 69.65; H, 5.84; N, 9.02%; found: C, 69.68; H, 5.85; N, 9.06%.

1-benzylidene-3-(5-oxo-1,5-diphenylpent-1-en-3-yl)thiourea (1h). Brown powder; mp: 111–114 °C; Yield: 80%; Water solubility: 0.40 mM/mL; IR(KBr) ν : 3175.53, 3070.50, 3032.28, 2597.48, 1714.10, 1624.38; ^1H NMR (300 MHz) δ 9.47(s, 1H), 9.26(s, 1H), 7.97–7.94(dd, $J=7.33$ Hz, $J=7.37$ Hz, 2H, Ar-ring), 7.86–7.84(dd, $J=7.31$ Hz, $J=7.35$ Hz, 2H), 7.63–7.59(d, 1H, $J=6.21$ Hz, Ar-ring), 7.53–7.51(2H, dd, $J=7.31$ Hz, $J=7.35$ Hz Ph), 7.50–7.44(3H, m, Ar-ring), 7.40–7.37(dd, $J=7.33$ Hz, $J=7.37$ Hz, 2H, Ar ring), 7.35–7.32(d, $J=6.21$ Hz, 1H, Ar ring), 7.26–7.24(dd, $J=7.31$ Hz, $J=7.35$ Hz, 2H, Ar ring), 6.56–6.54(d, $J=6.20$ Hz, 1H), 6.19–6.17(d, $J=6.21$ Hz, 1H), 3.84–3.82(m, 1H), 2.94–2.92(d, $J=6.21$ Hz, 2H); ^{13}C NMR (75 MHz): 197.4(1C), 182.0(1C), 136.7, 133.1, 128.8, 128.6(6C, Ph ring), 136.4, 128.6, 128.5, 127.9(6C, Ar ring), 135.2, 134.4, 116.1, 20.6 (6C, Ph ring), 134.6, 128.1, 55.6, 50.1, 14.4; EIMS(m/z): 399.15(M^+ , 27%); Anal. Calcd. for $\text{C}_{25}\text{H}_{22}\text{N}_2\text{O}\text{S}$: C, 75.35; H, 5.56; N, 7.03%; found: C, 75.30; H, 5.60; N, 7.04%.

1-(5-Oxo-1,5-diphenylpent-1-en-3-yl)-3-(3-phenylallylidene)thiourea (1i). Light yellow powder; mp: 276–279 °C; Yield: 87%; Water solubility: 0.10 mM/mL; IR(KBr) ν : 3174.23, 3069.30, 3031.68, 2598.98, 1715.70, 1626.38; $^1\text{H NMR}$ (300 MHz): δ 9.26(s, 1H), 7.98–9.96(dd, $J=7.33$ Hz, $J=7.37$ Hz, 2H), 7.65–7.63 (d, $J=6.21$ Hz, 1H), 7.62–7.59(dd, $J=7.31$ Hz, $J=7.35$ Hz, 2H), 7.56–7.54(dd, $J=7.31$ Hz, $J=7.35$ Hz, 2H), 7.52(s, 1H), 7.42–7.39 (dd, $J=7.33$ Hz, $J=7.37$ Hz, 4H, Ar ring), 7.31–7.27(d, $J=6.21$ Hz, 2H, Ar ring), 7.26–7.24(dd, $J=7.31$ Hz, $J=7.35$ Hz, 2H, Ar ring), 7.22–7.18(d, $J=6.21$ Hz, 1H, CH), 6.81–6.79(d, $J=6.23$ Hz, 1H), 6.56–6.52(d, $J=6.21$ Hz, 1H), 6.19–6.17(d, $J=6.21$ Hz, 1H, CH), 3.84–3.79(m, 1H), 2.94–6.92(d, $J=6.21$ Hz, 2H); $^{13}\text{C NMR}$ (75 MHz): 197.4 (1C), 189.3(1C), 163.7, 136.7, 133.1, 128.8, 128.6, (6C, Ph ring), 136.4, 128.6, 128.5, 127.9(6C, Ar ring), 135.2, 134.4, 116.1, 20.6(6C, Ph ring), 134.6, 132.9, 128.3, 119.9, 55.9, 50.6; EIMS(m/z) 425.16 (M^+ , 30%); Anal. Calcd. for $\text{C}_{27}\text{H}_{24}\text{N}_2\text{OS}$: C, 76.38; H, 5.70; N, 6.60%; found: C, 76.30; H, 5.74; N, 6.62%.

3-(Naphthalen-2-ylamino)-1,5-diphenylpent-4-en-1-one (1j). Dark yellow colour; mp: 101–104 °C; Yield: 88%; Water solubility: 0.32 mM/mL; IR(KBr) ν : 3174.63, 3069.70, 3031.48, 1715.50, 1626.48 cm^{-1} ; $^1\text{H NMR}$ (300 MHz): δ 9.26(s, 1H, NH), 7.97–7.94 (dd, $J=7.33$ Hz, $J=7.37$ Hz, 2H, Ph), 7.88–7.84 (d, $J=6.21$ Hz, 1H, Naphthyl), 7.83–7.81(d, $J=6.21$ Hz, 1H, Naphthyl), 7.77–7.74(d, $J=6.21$ Hz, 1H, Naphthyl), 7.49–7.45 (d, $J=6.21$ Hz, 1H, Naphthyl), 7.45–7.41 (d, $J=6.21$ Hz, 1H, Naphthyl), 7.50–7.48(dd, $J=7.31$ Hz, $J=7.35$ Hz, 2H, Naphthyl), 7.63–7.59(d, $J=6.23$ Hz, 1H, Ph), 7.53–7.50(dd, $J=7.31$ Hz, $J=7.35$ Hz, 2H, Ar-ring), 7.42–7.40 (dd, $J=7.33$ Hz, $J=7.37$ Hz, 2H, Ar ring), 7.35–7.33(d, $J=6.21$ Hz, 1H, Ar-ring), 7.25–7.21(dd, $J=7.31$ Hz, $J=7.35$ Hz, 2H, Ar ring), 6.56–6.54(d, $J=6.21$ Hz, 1H, CH), 6.19–6.17(d, $J=6.21$ Hz, 1H), 3.84–3.81(m, 1H), 2.90–2.87(d, $J=6.21$ Hz, 2H); $^{13}\text{C NMR}$ (75 MHz): 197.4(1C), 136.7, 133.1, 128.8, 128.6(6C, Ph ring), 136.4, 128.6, 128.5, 127.9(6C, Ar ring), 146.0, 133.7, 129.0, 126.8, 126.5, 125.3, 124.6, 121.4, 118.1, 104.5(10C, Naphthyl ring), 134.4, 128.1, 57.2, 50.5; EI-MS(m/z) 378.18 (M^+ , 29%); Anal. Calcd. for $\text{C}_{27}\text{H}_{23}\text{NO}$: C, 85.91; H, 6.14; N, 3.71%; found: C, 85.90; H, 6.10; N, 3.76%.

1,5-Diphenyl-3-(p-tolylamino)pent-4-en-1-one (1k). White powder; mp: 72–74 °C; Yield: 85%; Water solubility: 0.26 mM/mL; IR(KBr) ν : 3173.23, 3068.30, 3030.68, 1714.70, 1625.38; $^1\text{H NMR}$ (300 MHz): δ 9.28(s, 1H), 7.50(s, 1H, -CH), 7.97–7.96(dd, $J=7.35$ Hz, $J=7.39$ Hz, 2H, Ph), 7.64(d, $J=6.21$ Hz, 1H), 7.53(dd, $J=7.31$ Hz, $J=7.34$ Hz, 2H), 7.39(dd, $J=7.33$ Hz, $J=7.37$ Hz, 4H, Ar-ring), 7.33–7.31(d, $J=6.21$ Hz, 2H, Ar-ring), 7.24–7.20(dd, $J=7.31$ Hz, $J=7.35$ Hz, 2H, Ar-ring), 7.22–7.18(d, $J=6.21$ Hz, 1H), 7.01–6.98 (dd, $J=7.31$ Hz, $J=7.35$ Hz, 1H, Ph), 6.85–6.84(1H, d, $J=6.21$ Hz), 2.90–2.87 (d, $J=6.21$ Hz, 2H), 2.34(s, 3H); $^{13}\text{C NMR}$ (75 MHz): 197.4(1C), 136.7, 133.1, 128.8, 128.6(6C, Ph ring), 136.4, 128.6, 128.5, 127.9 (6C, Ar ring), 144.6, 129.8, 129.6, 113.4(6C, 4- CH_3 -Ph ring), 134.5, 128.6, 55.2, 50.6, 21.3; EIMS(m/z) 342.18(M^+ , 26%); Anal. Calcd. for $\text{C}_{24}\text{H}_{23}\text{NO}$: C, 84.42; H, 6.79; N, 4.10%; found: C, 84.30; H, 6.89; N, 4.12%.

N-(5-oxo-1,5-diphenylpent-1-en-3-yl)acetamide (1l). Pale yellow powder; mp: 122–124 °C; Yield: 84%; Water solubility: 0.15 mM/mL; IR(KBr) ν : 3170.23, 3065.30, 3027.68, 1711.70, 1622.38; $^1\text{H NMR}$ (300 MHz): δ 8.05(s, 1H, NH), 7.95–7.92 (dd, $J=7.31$ Hz, $J=7.36$ Hz, 2H, Ph), 7.65–7.64(d, $J=6.21$ Hz, 1H), 7.54–7.50(dd, $J=7.31$ Hz, $J=7.35$ Hz, 2H, Ar-ring), 7.38–7.34(dd, $J=7.31$ Hz, $J=7.35$ Hz, 1H, Ar ring), 7.31–7.28(d, $J=6.21$ Hz, 2H, Ar-ring), 7.25–7.21(dd, $J=7.31$ Hz, $J=7.35$ Hz, 2H, Ar ring), 6.56–6.53(d, $J=6.21$ Hz, 1H, CH), 6.17–6.15(d, $J=6.21$ Hz, 1H), 4.81–4.78 (m, 1H), 2.94–2.91(d, $J=6.21$ Hz, 2H), 1.84 (s, 3H); $^{13}\text{C NMR}$ (75 MHz): 197.4(1C), 170.7(1C), 136.7, 133.1, 128.8, 128.6(6C, Ph ring), 136.4, 128.6, 128.5, 127.9(6C, Ar ring), 134.1, 127.9, 48.4, 50.4, 23.7; EIMS(m/z) 294.14 (M^+ , 20%); Anal. Calcd. for $\text{C}_{19}\text{H}_{19}\text{NO}_2$: C, 77.79; H, 6.53; N, 4.77%; found: C, 77.80; H, 6.51; N, 4.75%.

N-(5-oxo-1,5-diphenylpent-1-en-3-yl)benzamide (1m). Brown powder; mp: 205–208 °C; Yield: 82%; Water solubility: 0.34 mM/mL; IR(KBr) ν : 3172.21, 3063.28, 3025.66, 1710.68, 1620.36; $^1\text{H NMR}$ (300 MHz): δ 8.41(s, 1H, NH), 8.03–7.96(dd, $J=7.33$ Hz, $J=7.37$ Hz, 2H, Ar-ring), 7.97(dd, $J=7.32$ Hz, $J=7.34$ Hz, 2H), 7.70–7.67(1H, d, $J=6.21$ Hz, Ar ring), 7.63–7.60(3H, m, Phenyl), 7.53–7.50(dd, $J=7.31$ Hz, $J=7.33$ Hz, 2H), 7.42–7.38 (dd, $J=7.33$ Hz, $J=7.37$ Hz, 4H, Ar ring), 7.33–7.30 (1H, d, $J=6.21$ Hz, Ph), 6.51–6.49(d, $J=6.21$ Hz, 1H), 6.19–6.17(d, $J=6.21$ Hz, 1H), 4.81–4.78(1H, m, -CH), 2.98–2.95(d, $J=6.21$ Hz, 2H); $^{13}\text{C NMR}$ (75 MHz): 197.4(1C), 167.5(1C), 136.7, 133.1, 128.8, 128.6, (6C, Ph ring), 136.4, 128.6, 128.5, 127.9 (6C, Ar ring), 134.2, 132.1, 128.8, 127.5 (6C, Ph ring), 135.1, 127.9, 49.2, 50.4; EIMS(m/z): 356.16 (M^+ , 26%); Anal. Calcd. for $\text{C}_{24}\text{H}_{21}\text{NO}_2$: C, 81.10; H, 5.96; N, 3.94%; found: C, 80.10; H, 5.92; N, 4.04%.

1-(5-Oxo-1,5-diphenylpent-1-en-3-yl)urea (1n). Pale green powder; mp: 260–262 °C; Yield: 82%; Water solubility: 0.40 mM/mL IR (KBr) ν : 3173.21, 3064.28, 3026.66, 1711.68, 1621.36; $^1\text{H NMR}$ (300 MHz): δ 9.22(s, 1H, NH), 8.83(s, 2H, NH_2), 7.97–7.94 (dd, $J=7.33$ Hz, $J=7.37$ Hz, 2H), 7.64–7.59 (m, 1H, Phenyl), 7.55–7.53(dd, $J=7.31$ Hz, $J=7.35$ Hz, 2H), 7.40–7.37(dd, $J=7.35$ Hz, $J=7.33$ Hz, 1H, Ar ring), 7.34–7.31(d, $J=6.21$ Hz, 2H, Ar ring), 7.23–7.18(dd, $J=7.31$ Hz, $J=7.35$ Hz, 2H, Ar ring), 6.56–6.54(d, $J=6.20$ Hz, 1H), 6.17–6.15(d, $J=6.21$ Hz, 1H), 4.81–4.78 (m, 1H), 2.94–2.91 (d, $J=6.21$ Hz, 2H); $^{13}\text{C NMR}$ (75 MHz): 197.4 (1C), 162.7 (1C), 136.7, 133.1, 128.8, 128.6, (6C, Ph ring), 136.4, 128.6, 128.5, 127.9(6C, Ar ring), 133.9, 128.9, 50.5, 49.9; EIMS(m/z): 295.14 (M^+ , 19%); Anal. Calcd. for $\text{C}_{18}\text{H}_{18}\text{N}_2\text{O}_2$: C, 73.45; H, 6.16; N, 9.52%; found: C, 73.40; H, 6.17; N, 9.54%.

1-Benzylidene-3-(5-oxo-1,5-diphenylpent-1-en-3-yl)urea (1o). Green solid; mp: 132–135 °C; Yield: 80%; Water solubility: 0.18 mM/mL; IR(KBr) ν : 3174.23, 3069.30, 3031.68, 2598.98, 1715.70, 1626.38; $^1\text{H NMR}$ (300 MHz): δ 9.48(s, 1H), 8.06 (s, 1H), 7.97(dd, $J=7.33$ Hz, $J=7.37$ Hz, 2H), 7.85–7.53(dd, $J=7.31$ Hz, $J=7.35$ Hz, 2H, Phenyl), 7.60–7.57 (dd, $J=7.31$ Hz, $J=7.35$ Hz, 1H), 7.63–7.60 (d, $J=6.21$ Hz, 1H, Phenyl), 7.55–7.52(dd, $J=7.31$ Hz,

$J=7.35$ Hz, 2H), 7.52 (m, 2H, Ph), 7.40–7.37(dd, $J=7.35$ Hz, $J=7.38$ Hz, 1H, Ar ring), 7.35–7.31(d, $J=6.21$ Hz, 2H, Ar ring), 7.27–7.23(dd, $J=7.31$ Hz, $J=7.35$ Hz, 2H, Ar ring), 6.56–6.54 (d, $J=6.21$ Hz, 1H), 6.19–6.16(d, $J=6.22$ Hz, 1H), 4.81–4.79 (m, 1H), 2.94 (d, $J=6.21$ Hz, 2H); ^{13}C NMR (75 MHz): 197.4(1C), 164.5 (1C), 163.7 (1C), 136.7, 133.1, 128.8, 128.6(6C, Ph ring), 136.4, 128.6, 128.5, 127.9 (6C, Ar ring), 133.7, 131.0, 129.2, 128.8(6C, Ph ring), 133.8, 127.7, 50.8, 49.9; EIMS(m/z): 383.17 (M^+ , 28%); Anal. Calcd. for $\text{C}_{25}\text{H}_{22}\text{N}_2\text{O}_2$: C, 78.51; H, 5.80; N, 7.32%; found: C, 78.50; H, 5.82; N, 7.31%.

1-(5-Oxo-1,5-diphenylpent-1-en-3-yl)-3-(3-phenylallylidene)urea (1p). White greenish powder; mp: 145–148 °C; Yield: 89%; Water solubility: 0.52 mM/mL; IR(KBr) ν : 3175.23, 3070.30, 3032.68, 2599.98, 1716.70, 1627.38; ^1H NMR (300 MHz): δ 8.04(s, 1H), 7.50(s, 1H), 7.96–7.93(dd, $J=7.33$ Hz, $J=7.37$ Hz, 2H, Ar-ring), 7.60–7.54(dd, $J=7.31$ Hz, $J=7.35$ Hz, 2H, Ar-ring), 7.64–7.59(d, $J=6.21$ Hz, 1H, Ph), 7.54–7.51(dd, $J=7.31$ Hz, $J=7.35$ Hz, 2H), 7.42–7.39(dd, $J=7.33$ Hz, $J=7.37$ Hz, 4H, Ar-ring), 7.32–7.28(d, $J=6.21$ Hz, 2H, Ar ring), 7.28–7.25 (dd, $J=7.31$ Hz, $J=7.35$ Hz, 2H, Ar ring), 7.24–7.21(d, $J=6.21$ Hz, 1H, CH), 6.85–6.83 (d, $J=6.21$ Hz, 1H), 6.54–6.51 (d, $J=6.21$ Hz, 1H, CH), 6.17–6.13(d, $J=6.21$ Hz, 1H, CH), 4.81–4.78 (m, 1H), 2.94–2.92 (d, $J=6.21$ Hz, 2H); ^{13}C NMR (75 MHz): 197.4(1C), 164.5(1C), 163.7 (1C), 136.7, 133.1, 128.8, 128.6(6C, Ph ring), 136.4, 128.6, 128.5, 127.9(6C, Ar ring), 135.2, 134.4, 116.1, 20.6(6C, Ph ring), 134.1, 133.5, 128.5, 119.9, 50.8, 49.9; EI-MS: 409.19 (M^+ , 29%); Elemental analysis: Anal. Calcd. for $\text{C}_{27}\text{H}_{24}\text{N}_2\text{O}_2$: C, 79.39; H, 5.92; N, 6.86%; found: C, 79.30; H, 5.96; N, 6.91%.

3-(Methylamino)-1,5-diphenylpent-4-en-1-one (1q). Light yellow powder; mp: 84–88 °C; Yield: 86%; Water solubility: 0.46 mM/mL; IR(KBr) ν : 3173.21, 3064.28, 3026.66, 1711.68, 1621.36; ^1H NMR(300 MHz) δ 9.26(s, 1H, NH), 7.97–7.94(dd, $J=7.31$ Hz, $J=7.36$ Hz, 2H, Ph), 7.68–7.62 (m, 1H, Ar-ring), 7.51–7.48(dd, $J=7.31$ Hz, $J=7.35$ Hz, 2H), 7.41–7.37(dd, $J=7.33$ Hz, $J=7.37$ Hz, 2H, Ar-ring), 7.31–7.29(d, $J=6.21$ Hz, 2H, Ar ring), 7.25–7.19(dd, $J=7.31$ Hz, $J=7.35$ Hz, 1H, Ar ring), 6.56–6.54 (d, $J=6.21$ Hz, 1H, CH), 6.19–6.17(d, $J=6.20$ Hz, 1H), 3.84–3.81 (m, 1H, –CH), 3.36(s, 3H), 2.79–2.77(d, $J=6.20$ Hz, 2H); ^{13}C NMR (75 MHz): 197.4(1C), 136.7, 133.1, 128.8, 128.6(6C, Ph ring), 136.4, 128.6, 128.5, 127.9(6C, Ar-ring), 134.6 (1C), 127.5, 57.1, 50.3, 23.1; EIMS(m/z): 266.15 (M^+ , 19%); Anal. Calcd. for $\text{C}_{18}\text{H}_{19}\text{NO}$: C, 81.47; H, 7.22; N, 5.28%; found: C, 81.40; H, 7.25; N, 5.32%.

Biological activities. *Larvicidal activity.* Larvicidal activity assessed to control the breed of mosquitoes at their larval stage by using chemical compounds as larvicides. Test compounds were deviated in various concentrations of 10, 25, 50 and 100 μM according to a method described previously¹⁶. Mortality caused by the compounds was assessed as ratios (%) of the numbers of dead vs. live larvae. The LD_{50} values were calculated using probit analysis.

Antifeedant activity. Antifeedant activity was evaluated to study the effect of larvicides against non-target aquatic species. The antifeedant activity was screened via 10, 25, 50 and 100 μM concentrations of the tested samples and evaluated for marine fingerlings (*O. mossambicus*). Mortality caused by the compounds was assessed as ratios (%) of the numbers of dead vs. live fingerlings. Table 4 summarizes the results. The method followed was described previously¹⁶.

Larval growth inhibition and regulation. The regulation and inhibition of larval growth in *C. quinquefasciatus* by compound **1i** (10 μM) were analysed via the water-immersion method⁶³.

Molecular docking. *Preparation of ligands.* The ligand molecules (**1a–1q**) were drawn via Chemdraw 12.0 and energy was minimized by using the MM2 force field in Chem3Dpro software. The ligand molecules were then saved in Protein Data Bank (PDB) format and further used for molecular docking studies.

Preparation of receptor. The 3D crystal structure of mosquito odorant binding protein (PDB ID: 3OGN) was downloaded from Protein Data Bank. The water molecules and inbound co-crystallized ligands were removed from the receptor using the Discovery Studio 2019 program. The receptor was energy minimized via the SWISS PDB Viewer program. The receptor was then used for molecular docking evaluation.

Identification of binding pocket. The binding pocket of the target protein was recognized by using inbound co-crystallized ligands via the Discovery Studio 2019 Program. Residues of the amino acids Tyr10, Leu15, Leu19, Leu73, Leu80, Met84, Ile87, Ala88, Met91, His111, Trp114, His121, and Phe123 were situated in the binding pocket.

Docking. The interaction of binding modes between compounds **1a–1q**, **permethrin**, **temephos** (see Supplementary Material) and the mosquito odorant binding protein was assessed using molecular docking studies via Autodock vina 1.1.2. software⁶⁴. The selection of docking grid box was based on the active amino acid residues situated on the binding pocket. The search grid of the 3OGN protein was stable with the dimensions sizes x: 22, y: 20, and z: 22 with center_x: 18.681, y: 49.66, and z: 11.409, with a spacing of 1.0 Å⁶⁵. The value of exhaustiveness was set to 8 and the interactions were visually examined using the Pymol and Discovery studio 2019 programs.

Molecular dynamics simulations. Gromacs 2020.1 version was used to carry out the Molecular dynamics simulation for docked complex structure of ligand **1i** with protein 3OGN to understand the stability of the docked

complexes. Ligand topology was generated using PRODRG server and it is combined with protein topology for making complex topology, the system was generated using force field GROMOS 43a1, solvated using a single point charge (SPC) water model. The system was framed by cubic box with a distance of 2 nm from the box to the surface of the protein.

The necessary ions were further added in order to neutralize the systems. The docked complex energy was minimized by energy minimization process using steepest descent algorithm, for each simulation, 50,000 steps were used for energy minimization. The LINCS algorithm was used to constrained the bond lengths and the electrostatics computed by PME method. NVT and NPT ensembles were used to equilibrating the systems for each 100 ps. The V-rescale thermostat was used for equilibration with a reference temperature of 300 K. Finally, the production MD run was approved for 10 ns with a time-step of 2 fs. Docked complex structure coordinates were hoarded every 10 ps and used for further analysis. The result was analysed through the RMSD, RMSF, gyration, hydrogen bonds plots and Xmgrace software was used for plotting graphs.

Statistical analysis. The LD₅₀ values was calculated based on at least three independent assessments and the standard deviations (SD) were calculated using Microsoft Excel.

Conclusions

In this study, we identified the most effective and easily prepared active larvicidal Mannich base synthesis derivatives using the grindstone method using Cu(II)-tyrosinase as a catalyst, which is economical and leads to good coating and high yield. These compounds were investigated for their use as larvicides against *Culex quinquefasciatus* and for their toxicity against non-target aquatic species through ichthyotoxic activity. A total of 17 compounds were screened, and compound **1i** was found to be the most active (LD₅₀ = 12.09 µM) against *Culex quinquefasciatus* compared to **Permethrin** (LD₅₀ = 54.6 µM). The compound **1i** was highly active compared to **Permethrin** > 10 differences compared with standard permethrin and also compound **1i** induced 0% mortality within 24 h against *Oreochromis mossambicus* in an antifeedant screening. Molecular docking was carried out with all compounds **1a–1q** and the controls **temephos** and **permethrin** against the 3OGN protein, and the resulting docking score was the best for compound **1i**. In conclusion, our results indicate that compound **1i** is the most effective insecticide and that the compounds outlined in this paper may serve as a prospective foundation for emerging ecologically significant bioactive compounds as well as eco-friendly pesticides and biopharmaceuticals.

Received: 27 February 2021; Accepted: 30 August 2021

Published online: 20 October 2021

References

- Toda, F., Tanaka, K. & Sekikawa, A. Host–guest complex formation by a solid–solid reaction. *J. Chem. Soc. Chem. Commun.* **4**, 279–280. <https://doi.org/10.1039/C39870000279> (1987).
- Mannich, C. Eine synthese von β-ketonbasen. *Arch. Pharm.* **255**, 261–276. <https://doi.org/10.1002/ardp.19172550217> (1917).
- Sanchez-Ferrer, A., Rodriguez-Lopez, J., Garcia-Canovas, F. & Garcia-Carmona, F. Tyrosinase: A comprehensive review of its mechanism. *Biochim. Biophys. Acta.* **1247**, 1–11. [https://doi.org/10.1016/0167-4838\(94\)00204-T](https://doi.org/10.1016/0167-4838(94)00204-T) (1995).
- Solomon, E. I., Sundaram, U. M. & Machonkin, T. E. Multicopper oxidases and oxygenases. *Chem. Rev.* **96**, 2563–2606. <https://doi.org/10.1021/cr950046o> (1996).
- Solomon, E. I., Chen, P., Metz, M., Lee, S. K. & Palmer, A. Oxygen binding, activation, and reduction to water by copper proteins. *Angew. Chem. Int. Ed. Engl.* **40**, 4570–4590. [https://doi.org/10.1002/1521-3773\(20011217\)40:24%3c4570](https://doi.org/10.1002/1521-3773(20011217)40:24%3c4570) (2001).
- Rolff, M., Schottenheim, J., Decker, H. & Tuzcek, F. Copper-O₂ reactivity of tyrosinase models towards external monophenolic substrates: Molecular mechanism and comparison with the enzyme. *Chem. Soc. Rev.* **40**, 4077–4098. <https://doi.org/10.1039/C0CS00202J> (2011).
- Quist, D. A., Diaz, D. E., Liu, J. J. & Karlin, K. D. Activation of dioxygen by copper metalloproteins and insights from model complexes. *J. Biol. Inorg. Chem.* **22**, 253–288. <https://doi.org/10.1007/s00775-016-1415-2> (2017).
- Hamann, J. D., Herzigkeit, B., Jurgeleit, R. & Tuzcek, F. Small-molecule models of tyrosinase: From ligand hydroxylation to catalytic monooxygenation of external substrates. *Coord. Chem. Rev.* **334**, 54–66. <https://doi.org/10.1016/j.ccr.2016.07.009> (2017).
- Gerdemann, C., Eicken, C. & Krebs, B. The crystal structure of catechol oxidase: New insight into the function of type-3 copper proteins. *Acc. Chem. Res.* **35**, 183–191. <https://doi.org/10.1021/ar990019a> (2002).
- van Holde, K. E. & Miller, K. I. Hemocyanins. *Adv. Protein Chem.* **47**, 1–81. [https://doi.org/10.1016/S0065-3233\(08\)60545-8](https://doi.org/10.1016/S0065-3233(08)60545-8) (1994).
- Manabe, K. & Kobayashi, S. Mannich-type reactions of aldehydes, amines, and ketones in a colloidal dispersion system created by a Bronsted Acid-Surfactant-combined catalyst in water. *Org. Lett.* **1**, 1965–1967. <https://doi.org/10.3390/insects7020025> (1999).
- Jing-Bo, Y., Gang, P., Zhi-Jiang, J., Zi-Kun, H. & Wei-Ke, S. Mechano-chemical oxidative Mannich reaction: evaluation of chemical and mechanical parameters for the mild and chemoselective coupling of N-tert-butoxycarbonyltetrahydroquinolines and ketones. *Eur. J. Org. Chem.* **22**, 5340–5344. <https://doi.org/10.1002/ejoc.201600987> (2016).
- Khanna, G., Aggarwal, K. & Khuran, J. L. An efficient and confluent approach for the synthesis of novel 3,4-dihydro-2H-naphtho [2,3-e] [1,3]oxazine-5,10-dione derivatives by a three component reaction in ionic liquid. *RSC Adv.* **5**, 46448–46454. <https://doi.org/10.1039/C5RA06169E> (2015).
- Ghomi, J. S. & Zahedi, S. Novel ionic liquid supported on Fe₃O₄ nanoparticles and its application as a catalyst in Mannich reaction under ultrasonic irradiation. *Ultrason Sonochem.* **34**, 916–923. <https://doi.org/10.1016/j.ultrsonch.2016.08.003> (2017).
- Ling-Ling, W., Yang, X., Da-Cheng, Y., Zhi, G. & Yan-Hong, H. Bio-catalytic asymmetric Mannich reaction of ketimines using wheat germ lipase. *Catal. Sci. Technol.* **6**, 3963–3970. <https://doi.org/10.1039/C5CY01923K> (2016).
- Abdel-Fattah Mostafa, A. *et al.* Synthesis of novel benzopyran- connected pyrimidine and pyrazole derivatives via a green method using Cu(II)-tyrosinase enzyme catalyst as potential larvicidal, antifeedant activities. *RSC Adv.* **9**, 25533–25543. <https://doi.org/10.1039/C9RA04496E> (2019).
- Georges, K., Jayaprakasam, B., Dalavoy, S. S. & Nair, M. G. Pestmanaging activities of plant extracts and anthraquinones from *Cassia nigricans* from Burkina Faso. *Bioresour. Technol.* **99**, 2037–2045. <https://doi.org/10.1016/j.biortech.2007.02.049> (2008).
- Govindarajan, M. Chemical composition and larvicidal activity of leaf essential oil from *Clausena anisata* (Willd.) Hook. f. ex Benth (Rutaceae) against three mosquito species. *Asian Pac. J. Trop. Med.* **3**, 874–887. [https://doi.org/10.1016/S1995-7645\(10\)60210-6](https://doi.org/10.1016/S1995-7645(10)60210-6) (2010).

19. Methoprene: General Fact Sheet. *National Pesticide Information Center*. Accessed 12 Feb 2016.
20. Bazaes, A., Olivares, J. & Schmachtenberg, O. Properties, projections, and tuning of teleost olfactory receptor neurons. *J. Chem. Ecol.* **39**, 451–464. <https://doi.org/10.1007/s10886-013-0268-1> (2013).
21. De March, C. A. & Golebiowski, J. A. A computational microscope focused on the sense of smell. *Biochimie* **107**, 3–10. <https://doi.org/10.1016/j.biochi.2014.06.006> (2014).
22. Pechlaner, M. & Oostenbrink, C. Multiple binding poses in the hydrophobic cavity of bee odorant binding protein AmelOBP14. *J. Chem. Inform. Model.* **55**, 2633–2643. <https://doi.org/10.1021/acs.jcim.5b00673> (2015).
23. Leal, W. S. *et al.* Reverse and conventional chemical ecology approaches for the development of oviposition attractants for *Culex* mosquitoes. *PLoS ONE* **3**(8), e3045. <https://doi.org/10.1371/journal.pone.0003045> (2008).
24. de Brito, N. F., Moreira, M. F. & Melo, C. A. A look inside odorant-binding proteins in insect chemoreception. *J. Insect Physiol.* **95**, 51–65. <https://doi.org/10.1016/j.jinsphys.2016.09.008> (2016).
25. Chu, W. T. *et al.* Constant pH molecular dynamics (CpHMD) and molecular docking studies of CquiOBP1 pH-induced ligand releasing mechanism. *J. Mol. Model.* **19**, 1301–1309. <https://doi.org/10.1007/s00894-012-1680-0> (2013).
26. Agnieszka, C. *et al.* Current research on the safety of pyrethroids used as insecticides. *Medicina* **54**, 61. <https://doi.org/10.3390/medicina54040061> (2018).
27. Kumar, S., Kaushik, G. & Villarreal-Chiu, J. F. Scenario of organophosphate pollution and toxicity in India: A review. *Environ. Sci. Pollut. Res.* **23**, 9480–9949. <https://doi.org/10.1007/s11356-016-6294-0> (2016).
28. Peiris, H. T. R. & Hemingway, J. Effect of fenthion treatment on larval densities of insecticide-resistant *Culex quinquefasciatus* in an urban area of Sri Lanka. *Med. Vet. Entomol.* **10**, 283–287. <https://doi.org/10.1111/j.1365-2915.1996.tb00744.x> (1996).
29. Amel, I. O. & Manal, A. H. Curcumin mitigates fenthion-induced testicular toxicity in rats: Histopathological and immunohistochemical study. *Afr. Zool.* **52**, 3–4. <https://doi.org/10.1080/15627020.2017.1396194> (2017).
30. Mense, S. M. *et al.* The common insecticides cyfluthrin and chlorpyrifos alter the expression of a subset of genes with diverse functions in primary human astrocytes. *Toxicol. Sci.* **93**, 125–135. <https://doi.org/10.1093/toxsci/kt046> (2006).
31. Mie, A., Rudén, C. & Grandjean, P. Safety of Safety Evaluation of Pesticides: Developmental neurotoxicity of chlorpyrifos and chlorpyrifos-methyl. *Environ. Health.* **17**, 77. <https://doi.org/10.1186/s12940-018-0421-y> (2018).
32. Liu, J. *et al.* Toxicity assessment of chlorpyrifos-degrading fungal bio-composites and their environmental risks. *Sci. Rep.* **8**, 2152. <https://doi.org/10.1038/s41598-018-20265-9> (2018).
33. Pierce, R. H., Henry, M. S., Kelly, D. & Kozlowski, W. Hazard assessment of temephos applied to a southwest Florida, USA, salt marsh community. *Environ. Toxicol. Chem.* **19**, 501–507. <https://doi.org/10.1002/etc.5620190232> (2000).
34. Pinkney, A. E. *et al.* Effects of the mosquito larvicides temephos and methoprene on insect populations in experimental ponds. *Environ. Toxicol. Chem.* **19**, 678–684. <https://doi.org/10.1002/etc.5620190320> (2000).
35. Wade, A., Lin, C. H., Kurkul, C., Regan, E. R. & Johnson, R. M. Combined toxicity of insecticides and fungicides applied to California almond orchards to honey bee larvae and adults. *Insects* **10**, 20. <https://doi.org/10.3390/insects10010020> (2019).
36. Liu, S. S., Arthur, F. H., Vangundy, D. & Phillips, T. W. Combination of methoprene and controlled aeration to manage insects in stored wheat. *Insects* **7**, 25. <https://doi.org/10.3390/insects7020025> (2016).
37. Park, I. K. *et al.* Larvicidal activity of lignans identified in *Phryma leptostachya* Var. asiatica roots against tree mosquito species. *J. Agric. Food. Chem.* **53**, 969–972. <https://doi.org/10.1021/jf048208h> (2005).
38. Yang, J. Y. *et al.* Constituents of volatile compounds derived from *Melaleuca alternifolia* leaf oil and acaricidal toxicities against house dust mites. *J. Korean Soc. App. Biol. Chem.* **56**, 91–94. <https://doi.org/10.1007/s13765-012-2195-1> (2013).
39. Pasquale, G. *et al.* Quantitative structure–activity relationships of mosquito larvicidal chalcone derivatives gustavo pasquale. *J. Agric. Food. Chem.* **60**, 692–697. <https://doi.org/10.1021/jf203374r> (2012).
40. Targanski, S. K. *et al.* Larvicidal activity of substituted chalcones against *Aedes aegypti* (Diptera: Culicidae) and non-target organisms. *Pest Manag. Sci.* **77**, 325–334. <https://doi.org/10.1002/ps.6021> (2020).
41. Schafer, E. W. Jr. & Bowles, W. A. Jr. Acute oral toxicity and repellency of 933 chemicals to house and deer mice. *Arch. Environ. Contain. Toxicol.* **14**, 111–129. <https://doi.org/10.1007/BF01055769> (1985).
42. Bowman, L. R., Donegan, S. & McCall, P. J. Is dengue vector control deficient in effectiveness or evidence? Systematic review and metaanalysis. *PLoS Negl. Trop. Dis.* **10**(1), e0004551–e4624. <https://doi.org/10.1371/journal.pntd.0004551> (2016).
43. Nkya, T. E., Akhouayri, I., Kisinza, W. & David, J. P. Impact of environment on mosquito response to pyrethroid insecticides: Facts, evidences and prospects. *Insect. Biochem. Mol. Biol.* <https://doi.org/10.1016/j.ibmb.2012.10.006407-416> (2013).
44. Jayaraj, R., Megha, P. & Sreedev, P. Review article: Organochlorine pesticides, their toxic effects on living organisms and their fate in the environment. *Interdiscip. Toxicol.* **9**, 90–100. <https://doi.org/10.1515/intox-2016-0012> (2016).
45. Gross, A. D. *et al.* Toxicity and synergistic activities of chalcones against *Aedes aegypti* (Diptera: Culicidae) and *Drosophila melanogaster* (Diptera: Drosophilidae). *J. Med. Entomol.* **54**, 382–386. <https://doi.org/10.1093/jme/tjw183> (2018).
46. Lee, S. H. *et al.* Insect growth regulatory and larvicidal activity of chalcones against *Aedes albopictus*. *Entomol. Res.* **48**, 55–59. <https://doi.org/10.1111/1748-5967.12288> (2018).
47. Satyavani, S. R., Kanjilal, S., Rao, M. S., Prasad, R. B. N. & Murthy, U. S. N. Synthesis and mosquito larvicidal activity of furanochalcones and furanoflavonoids analogous to karanjin. *Med. Chem. Res.* **24**, 842–850. <https://doi.org/10.1007/s00044-014-1160-4> (2015).
48. Vesely, J. & Rios, R. Enantioselective methodologies using *N*-carbamoyl-imines. *Chem. Soc. Rev.* **43**, 611–630. <https://doi.org/10.1039/C3CS60321K> (2014).
49. Gul, H. I., Demirtas, A., Ucar, G., Taslimi, P. & Gulcin, I. Synthesis of Mannich bases by two different methods and evaluation of their acetylcholine esterase and carbonic anhydrase inhibitory activities. *Lett. Drug Design Discov.* **14**, 573–580 (2017).
50. Sivakumar, K. K., Rajasekaran, A., Senthilkumar, P. & Wattamwar, P. P. Conventional and microwave assisted synthesis of pyrazolone Mannich bases possessing anti-inflammatory, analgesic, ulcerogenic effect and antimicrobial properties. *Bioorg. Med. Chem. Lett.* **24**, 2940–2944. <https://doi.org/10.1016/j.bmcl.2014.04.067> (2014).
51. Branneby, C., Carlqvist, P., Hult, K., Brinck, T. & Berglund, P. Aldol additions with mutant lipase: Analysis by experiments and theoretical calculations. *J. Mol. Catal. B* **31**, 123–12838. <https://doi.org/10.1016/j.molcatb.2004.08.005> (2004).
52. Dindulkar, S. D., Puranik, V. G. & Jeong, Y. T. Supported copper triflate as an efficient catalytic system for the synthesis of highly functionalized 2-naphthol Mannich bases under solvent free condition. *Tetrahedron Lett.* **53**, 4376–4380. <https://doi.org/10.1016/j.tetlet.2012.06.022> (2012).
53. Zhang, H. J., Xie, Y. C. & Yin, L. Copper(I)-catalyzed asymmetric decarboxylative Mannich reaction enabled by acidic activation of 2H-azirines. *Nat. Commun.* **10**, 1699. <https://doi.org/10.1038/s41467-019-09750-5> (2019).
54. Singh, S. K., Chandna, N. & Jain, N. *N*-Mannich bases of aromatic heterocyclic amides: Synthesis via copper-catalyzed aerobic cross-dehydrogenative coupling under ambient conditions. *Org. Lett.* **19**, 1322–1325. <https://doi.org/10.1021/acs.orglett.7b00125> (2017).
55. Kidwai, M., Mishra, N. K., Bansal, V., Kumar, A. & Mozumdar, S. Novel one-pot Cu-nanoparticles-catalyzed Mannich reaction. *Tetrahedron Lett.* **50**, 1355–1358. <https://doi.org/10.1016/j.tetlet.2009.01.031> (2009).
56. Chai, S. J., Lai, Y. F., Zheng, H. & Zhang, P. F. A novel trypsin-catalyzed three-component Mannich reaction. *Helv. Chim. Acta.* **93**, 2231–2236. <https://doi.org/10.1002/hlca.201000063> (2010).
57. Li, K. *et al.* Lipase-catalysed direct Mannich reaction in water: utilization of biocatalytic promiscuity for C-C bond formation in a “one-pot” synthesis. *Green. Chem.* **11**, 777–779. <https://doi.org/10.1039/B817524A> (2009).

58. Xue, Y. *et al.* Protease-catalysed direct asymmetric mannich reaction in organic solvent. *Sci. Rep.* **2**, 761. <https://doi.org/10.1038/srep00761> (2012).
59. Kano, T., Sakamoto, R., Akakura, M. & Maruoka, K. Stereocontrolled synthesis of vicinal diamines by organocatalytic asymmetric mannich reaction of *N*-protected aminoacetaldehydes: Formal synthesis of (–)-Agelastatin A. *J. Am. Chem. Soc.* **134**, 7516–7520. <https://doi.org/10.1021/ja301120z> (2012).
60. Arteaga, F. A. *et al.* Direct catalytic asymmetric mannich-type reaction of alkylamides. *Org. Lett.* **18**, 2391–2394. <https://doi.org/10.1021/acs.orglett.6b00879> (2016).
61. Kanazawa, A. M., Denis, J. N. & Greene, A. E. Highly stereocontrolled and efficient preparation of the protected, esterification-ready docetaxel (taxotere) side chain. *J. Org. Chem.* **59**, 1238–1240. <https://doi.org/10.1021/jo00085a004> (1994).
62. Chen, C. D. *et al.* Laboratory bioefficacy of nine commercial formulations of temephos against larvae of *Aedes aegypti* (L.), *Aedes albopictus* Skuse and *Culex quinquefasciatus* Say. *Trop. Biomed.* **26**, 360–365 (2009).
63. Song, G. P. *et al.* Synthesis and larvicidal activity of novel thenoylhydrazide derivatives. *Sci. Rep.* **6**, 22977–22990. <https://doi.org/10.1038/srep22977> (2016).
64. Trott, O. & Olson, A. J. AutoDock Vina: Improving the speed and accuracy of docking with a new scoring function, efficient optimization and multithreading. *J. Comput. Chem.* **31**, 455–461. <https://doi.org/10.1002/jcc.21334> (2010).
65. Abreu, R. M. V., Froufe, H. J. C., Queiroz, M. R. P., Isabel, C. F. R. & Ferreira, I. C. F. R. Selective flexibility of side-chain residues improves VEGFR-2 docking score using AutoDock Vina. *Chem. Biol. Drug. Des.* **79**, 530–534. <https://doi.org/10.1111/j.1747-0285.2011.01313.x> (2012).

Acknowledgements

This work was funded by Researchers Supporting Project number (RSP-2021/27), King Saud University, Riyadh, Saudi Arabia.

Author contributions

C.S. Synthesis of compounds and docking result analysis; D.A. Design the biological experiment; S.A. Methodology of biological activity analysis; G.R. Biological data analysis Molecular dynamics simulation studies; R.S. chemical data analysis; A.I. Investigation total work chemistry and Biology. All authors were contributing through writing—original draft.

Competing interests

The authors declare no competing interests.

Additional information

Supplementary Information The online version contains supplementary material available at <https://doi.org/10.1038/s41598-021-98281-5>.

Correspondence and requests for materials should be addressed to I.A.

Reprints and permissions information is available at www.nature.com/reprints.

Publisher's note Springer Nature remains neutral with regard to jurisdictional claims in published maps and institutional affiliations.



Open Access This article is licensed under a Creative Commons Attribution 4.0 International License, which permits use, sharing, adaptation, distribution and reproduction in any medium or format, as long as you give appropriate credit to the original author(s) and the source, provide a link to the Creative Commons licence, and indicate if changes were made. The images or other third party material in this article are included in the article's Creative Commons licence, unless indicated otherwise in a credit line to the material. If material is not included in the article's Creative Commons licence and your intended use is not permitted by statutory regulation or exceeds the permitted use, you will need to obtain permission directly from the copyright holder. To view a copy of this licence, visit <http://creativecommons.org/licenses/by/4.0/>.

© The Author(s) 2021